DUDLEY KNOX LIBRARY
NAVAL POSTGRADUATE SCHOOL
MONTEREY, CALIFORNIA 93943-5002

NAVAL POSTGRADUATE SCHOOL
Monterey, California

THESIS

THE RADIATION EFFECTS OF HIGH ENERGY ELECTRONS UPON THERMIONIC INTEGRATED CIRCUITS

by

William R. Arguello

December 1985

Thesis Advisor: F. R. Buskirk

Approved for public release; distribution is unlimited

T224633

URITY CLASSIFICATION OF THIS PAGE

REPORT DOCUMENTATION PAGE

REPORT SECURITY CLASSIFICATION	1b. RESTRICTIVE MARKINGS
SECURITY CLASSIFICATION AUTHORITY	3. DISTRIBUTION / AVAILABILITY OF REPORT Approved for public release; distribution is unlimited
DECLASSIFICATION / DOWNGRADING SCHEDULE	
PERFORMING ORGANIZATION REPORT NUMBER(S)	5. MONITORING ORGANIZATION REPORT NUMBER(S)

NAME OF PERFORMING ORGANIZATION val Postgraduate School	6b. OFFICE SYMBOL *(If applicable)* 61	7a. NAME OF MONITORING ORGANIZATION Naval Postgraduate School
ADDRESS *(City, State, and ZIP Code)* nterey, California 93943-5100		7b. ADDRESS *(City, State, and ZIP Code)* Monterey, California 93943-5100
NAME OF FUNDING / SPONSORING ORGANIZATION	8b. OFFICE SYMBOL *(If applicable)*	9. PROCUREMENT INSTRUMENT IDENTIFICATION NUMBER
ADDRESS *(City, State, and ZIP Code)*		10. SOURCE OF FUNDING NUMBERS

PROGRAM ELEMENT NO	PROJECT NO	TASK NO	WORK UNIT ACCESSION NO.

TITLE *(Include Security Classification)*
IE RADIATION EFFECTS OF HIGH ENERGY ELECTRONS UPON THERMIONIC INTEGRATED RCUITS

PERSONAL AUTHOR(S)
guello, William R.

TYPE OF REPORT	13b TIME COVERED	14 DATE OF REPORT *(Year, Month, Day)*	15 PAGE COUNT
ster's Thesis	FROM _____ TO _____	1985 December	74

SUPPLEMENTARY NOTATION

COSATI CODES			18. SUBJECT TERMS *(Continue on reverse if necessary and identify by block number)*
FIELD	GROUP	SUB-GROUP	Thermionic Integrated Circuit (TIC); Radiation effects; Radiation dose

ABSTRACT *(Continue on reverse if necessary and identify by block number)*

Thermionic Integrated Circuit (TIC) devices use a hybrid of vacuum ube and integrated circuit technology. The integrated circuitry is abricated on a sapphire (Al_2O_3) substrate. A device was irradiated to ttempt to establish a total dose (measured in rad Si) of radiation to ause the TIC device to malfunction. The TIC device was irradiated using 0 and 100 Mev electrons provided by the Naval Postgraduate School Linear ccelerator (LINAC). The device received a total dose of 1.8155×10^9 rad i during the course of the experiments. It continued to function norm- lly throughout thr irradiation study, so it is concluded that the device s not sensitive to radiation, at least at the levels used.

DISTRIBUTION / AVAILABILITY OF ABSTRACT	21. ABSTRACT SECURITY CLASSIFICATION
☐ UNCLASSIFIED/UNLIMITED ☒ SAME AS RPT ☐ DTIC USERS	Unclassified

NAME OF RESPONSIBLE INDIVIDUAL	22b TELEPHONE *(Include Area Code)*	22c. OFFICE SYMBOL
of. Fred R. Buskirk	(408) 646-2765	Code 61Bs

FORM 1473, 84 MAR — 83 APR edition may be used until exhausted. All other editions are obsolete. SECURITY CLASSIFICATION OF THIS PAGE

Approved for public release; distribution is unlimited.

The Radiation Effects of High Energy Electrons upon Thermionic Integrated Circuits

by

William R. Arguello
Lieutenant, United States Navy
B.S., University of Utah 1977

Submitted in partial fulfillment of the
requirements for the degree of

MASTER OF SCIENCE IN PHYSICS

from the

ABSTRACT

Thermionic Integrated Circuit (TIC) devices use a hybrid of vacuum tube and integrated circuit technology. The integrated circuitry is fabricated on a sapphire (Al_2O_3) substrate. A device was irradiated to attempt to establish a total dose (measured in rad Si) of radiation to cause the TIC device to malfunction. The TIC device was irradiated using 30 and 100 Mev electrons provided by the Naval Postgraduate School Linear Accelerator (LINAC). The device received a total dose of 1.8155×10^9 rad Si during the course of the experiments. It continued to function normally throughout the irradiation study, so it is concluded that the device is not sensitive to radiation, at least at the levels used.

TABLE OF CONTENTS

I. INTRODUCTION 7

A. BACKGROUND 7

B. TIC DEVICE 10

C. RADIATION TYPES AND SOURCES 10

II. THEORY 14

A. TIC DEVICE OPERATION 14

B. HIGH ENERGY ELECTRON INTERACTION IN MATERIAL 18

1. Photon Interaction In Material 21

C. ELECTRON PRODUCTION OF FRENKEL PAIRS 23

D. STOPPING POWER 29

III. EXPERIMENT 34

A. DEVICE FABRICATION 34

B. NPS LINAC 42

D. EXPERIMENTAL PROCEDURE 44

1. Pre-irradiation Measurements 44

2. Pre-irradiation Procedure 47

3. Test Procedure 49

IV. DATA AND RESULTS 52

A. BASELINE DATA 52

B. IRRADIATION 52

C. COMPUTING THE DOSE 53

D. RESULTS OF IRRADIATION 57

E. STRUCTURAL FAILURE OF THE DEVICE 60

DUDLEY KNOX LIBRARY
NAVAL POSTGRADUATE SCHOOL
MONTEREY, CALIFORNIA 93943-5002

F. PREVIOUS RADIATION STUDIES_____ 64

G. RADIATION HARDNESS OF TYPICAL MICROCIRCUITS____ 64

V. CONCLUSIONS_____ 67

A. RESULTS OF RADIATION STUDIES_____ 67

APPENDIX: EQUIPMENT LIST_____ 70

LIST OF REFERENCES_____ 71

INITIAL DISTRIBUTION LIST_____ 73

ACKNOWLEDGEMENT

I would like to thank professor Fred Buskirk for his assistance and interest in this thesis project.

The E-11 group at Los Alamos National Laboratory particularly, Dave Lynn, Dale Wilde and Rich Dooley receive my deepest gratitude. The assistance and direction they provided were invaluable in the completion of this thesis.

Many thanks go to Don Snyder for working wonders in keeping the LINAC running until the experiments were completed.

Thank you to Lcdr. Robert "DOC BOB" Pornaras for all of the assistance you gave me in completing this theis.

I. INTRODUCTION

A. BACKGROUND

The core of present day and future weapons systems, satellite communications systems and operational space systems is the semiconductor integrated circuit. The low power requirements, miniaturization and speed of these devices have allowed the developement of ballistic missles and satellite systems. The shortcoming of solid state devices is their susceptibility to failure when operating in nuclear or space radiation environments. Many projects are currently underway to develop "hardening techniques" (hardening refers to making a device less susceptible to damage or upset from radiation) to increase the reliability of solid state circuitry in high radiation environments.

The Thermionic Integrated Circut (TIC) device which is currently being developed and tested by D. Lynn. J. B. McCormic et al. at Los Alamos National Laboratory shows great promise as a method of hardening solid state circuits. TIC devices are constructed using a hybrid of vacuum tube and integrated circuit technology. Figure 1-1 shows the package of the TIC device. The glass vacuum tube suoports the necessary internal circuitry. The TIC device

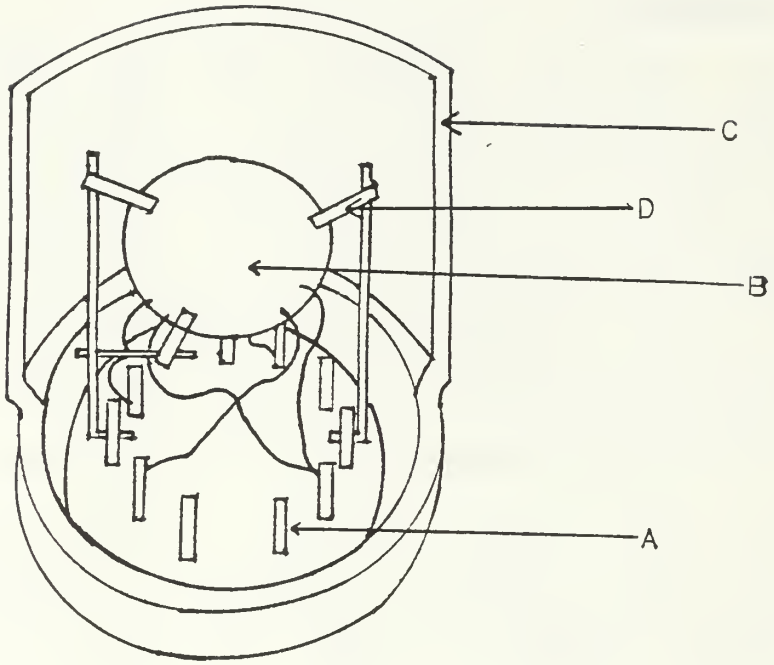

Figure 1-1. Structure of the TIC Triode

A. Pin connections for internal circuitry

B. Sapphire Substrate

C. Glass vacuum bulb

D. Bond strap and support structure

The sapphire substrates support the integrated circuitry of the device.

incorperates photolithographically delineated thin films on sapphire (Al_2O_3) substrates [Ref. 1].

TIC devices could be used in conjunction with solid state devices to increase the survivablity of crucial systems operating in high radiation environments. Present projections call for TIC devices to reach the small to medium scale integration levels.

Previous radiation studies conducted at Los Alamos National Laboratory using neutrons, high energy photons, and protons demonstrated the ability of TIC devices to survive in high radiation environments. When the results of these studies were compared to present day semiconductor devices, the results showed TIC devices can survive orders of magnitude more radiation without damage. [Ref. 1].

The focus of this thesis is the radiation effects of high energy (30-100 Mev) electrons on a TIC device. The source of electrons is the Naval Postgraduate School Linear Accelerator (LINAC). The discussion will be limited to the radiation damage effects on a simple TIC triode device after interaction with the high energy electrons. Electron interactions with the individual components (i.e., glass bulb, pins, cathode material etc.) of the device will not be discussed. Previous studies at Los Alamos have shown the individual component interaction with various radiation sources to have a negligible effect on device operation [Ref.1].

B. TIC DEVICE

Figure 1-1 shows the package of the TIC device and the internal structure. The internal structure is encased in a vacuum tube which is either entirely made of metal or a combination of glass and metal. Figures 1-2 and 1-3 show the fabricated integrated circuitry on the sapphire substrate. The structure of a single TIC integrated circuit for this typical triode is shown in figure 1-3. The grid, cathode and annode nomenclature is simular to that of a normal triode tube. Before inputting a signal the device heaters must raise the temperature of the substrate to between 973 and 1173 K.

Proposed uses of TIC devices are logic circuits in conjuction with solid state circuitry to ensure the survivability of any crucial systems operating in high radiation environments [Ref. 1].

C. RADIATION TYPES AND SOURCES

A TIC device used as a part of a logic circuit could be exposed to various sources of radiation. Different sources produce differnt types of radiation and each type of radiation damages the material with which it interacts in a different mannner.

Four high radiation environments in which TIC logic circuits may someday operate are: nuclear weapons radiation, nuclear reactor monitoring devices, cosmic radiation and the

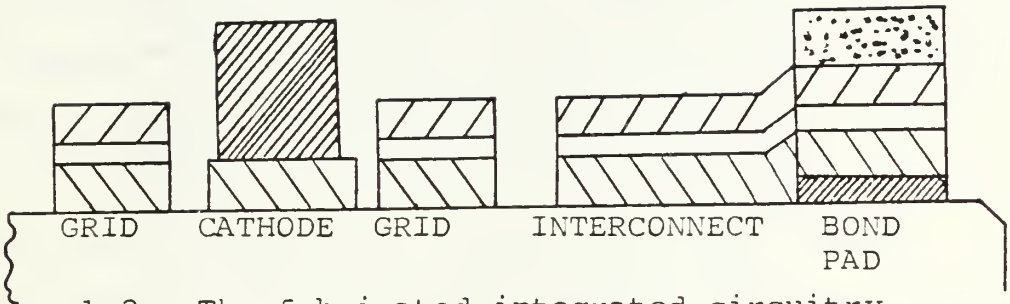

Figure 1-2. The fabricated integrated circuitry

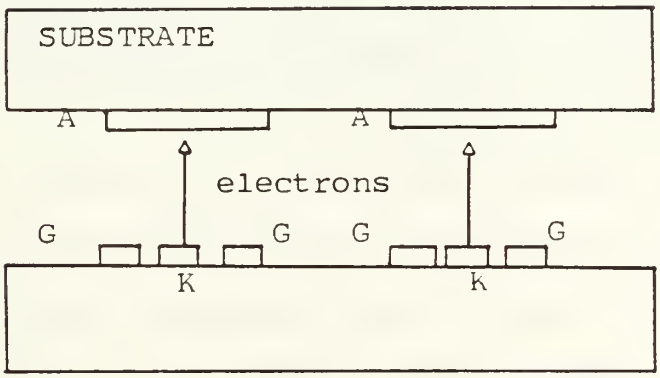

Figure 1-3. Grid (G), Cathode (K), and Anode (A) structure of the TIC device

Van Allen radiation Belt. All of these radiations sources are potentially lethal to present solid state circuitry.

The energy spectrum of a nuclear weapon produces several forms of radiation. The typical energy partition of the output of a weapon is: 50-80% X-ray production, 10-20% kinetic energy of fisson fragments and debris (including ions and electrons), 1% into neutrons and 0.5% into gamma ray production [Ref. 2].

Nuclear reactors produce neutrons, X-rays, and gamma rays. Reactor shielding is designed to prevent radiation from escaping outside of the containment vessel. In the event of a loss of cooling accident monitoring devices inside the containment vessel must be able to withstand a total dose of up to 1.36×10^{7} rad (air) over a 30 day period [Ref.3]. This high radiation environment requires some hardening technique to ensure full operation of the solid state monitoring devices.

In the space environment, high energy cosmic rays are the source of radiation. These charged particles (protons and electrons) have kinetic energies ranging from a few Mev to 100 Bev. The Van Allen Belt is a region of charged particles trapped by the earths magnetic field. Space systems operating in this region must withstand constant bombardment of charged particles in the Mev range.

The damage to material by neutrons, X-rays, high energy electrons, gamma rays or protons depends upon

several factors. The fluence (energy/cm^2.) and the flux (energy/cm^2. sec.) are functions of distance from the source of the radiation. The energy deposited in the material (measured in rads) is a function of the flux and the stopping power of the material. The theory portion of this thesis deals in much greater depth with the meanings and calculations of the above mentioned terms.

II. THEORY

A. TIC DEVICE OPERATION

The TIC device used in this experiment is shown in Figure 2-1. Figure 2-2 shows an individual integrated circuit of a TIC device [Ref. 1]. The grid (G) and cathode (K) are shown on the lower sapphire substrate. The anode (A) is on the upper sapphire substrate. To activate the device the substrate is heated to approximately 1023 K. The cathode emits electrons, the anode collects the electrons and the grid provides the gain by modulating the electron flow. The inputs to the substrate heater, cathode, and grid as well as the output from the anode are provided via the pins at the bottom of the vacuum tube (see Figure 1-1). The v-i charecteristics of this vacuum triode prior to radiation are shown in Figure 2-3.

A TIC device has operating characteristics that are very similar to those of a conventional vacuum triode. When a TIC device is used as an integrated circuit it can be affected by parasitic electrostatic interactions. These interactions can modify the expected device current [Ref. 1]. Figure 2-4 illustrates the type of undesirable electrostatic interactions that can modify the expected device current. Extraneous currents can be produced by resistive leakage from element to element. Spurious

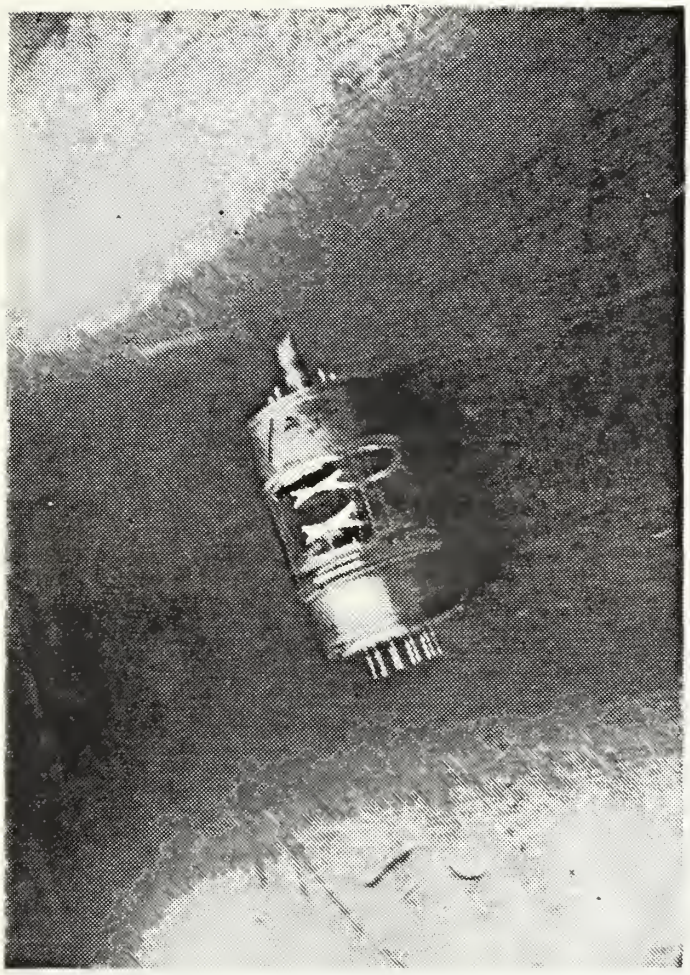

Figure 2-1. TIC device as used in the irradiation experiments.

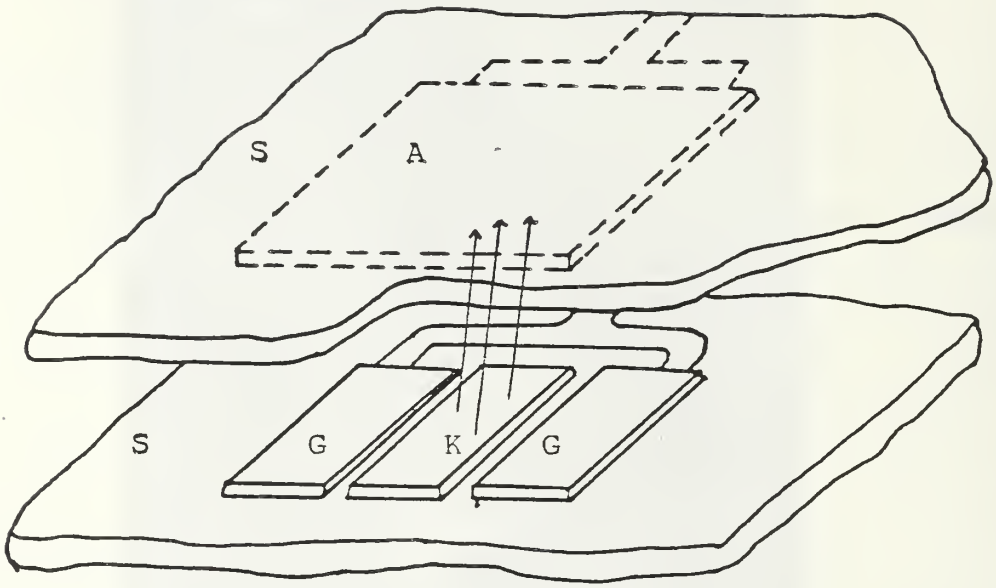

Figure 2-2. Electron flow for a vertical gain device.

A. Deposited anode

G. Thin metal grid

K. Coated cathode

The seperation between the grid and the cathode is 7.5 microns. The seperation between substrates is 1mm. The width of the grids and the cathode is 25 microns.

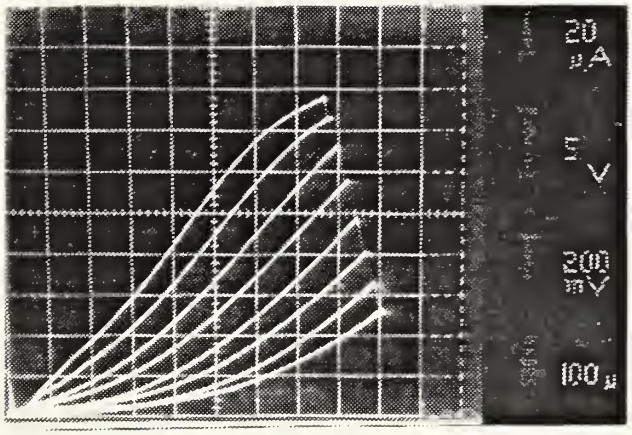

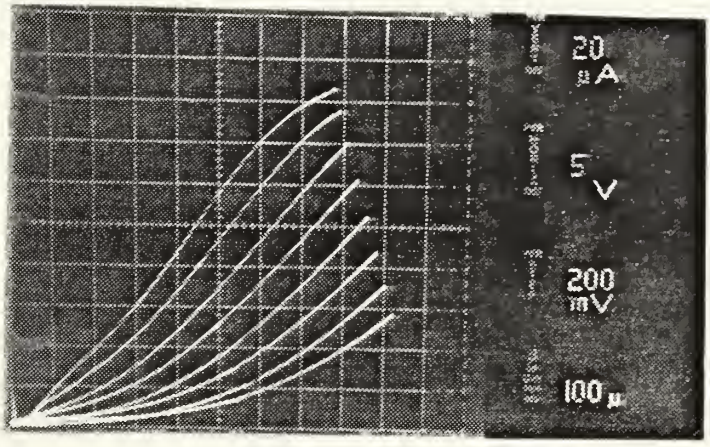

Figure 2-3. Photographs of the TIC device characteristics prior to irradiation. The device output was connected to a Textronix 576 curve tracer. The upper photograph was taken after two hours of warm-up time. The lower photograph was after eight hours of warm-up.

emissions from elements not designed to emit, such as grids, anodes and sheilds, can also affect device operation and performance.

For proper operation the grid cathode structure (GK1) of a particular device should not have its electric field at the surface appreciably altered by potentials applied to a neighboring grid cathode structure (GK2), or a neighboring shield anode (SA) (see Figure 2-5). Electrons are confined to the proper cathode anode path by the use of proper shield potential [Ref. 1].

A problem with the TIC device used in this thesis study was the slow poisoning of the cathode. The cathode poisoning is caused by argon gas used during the manufacture of the integrated circuits on the sapphire substrate (see section III. Triode Fabrication for further details). The electron emission from the cathode of a TIC device manufactured using the sputter etch process will steadily decrease and finally stop due to cathode poisoning [Ref. 4].

B. HIGH ENERGY ELECTRON INTERACTION IN MATERIAL

High energy electrons interacting with material cause excitation and ionization of the atoms in the material. Sapphire (Al_2O_3) is a crystalline material, therefore, the atoms are arranged in a regular, repetitive, gridlike pattern known as a lattice. Excitation occurs when the electrons of the lattice atoms absorb sufficient quantities

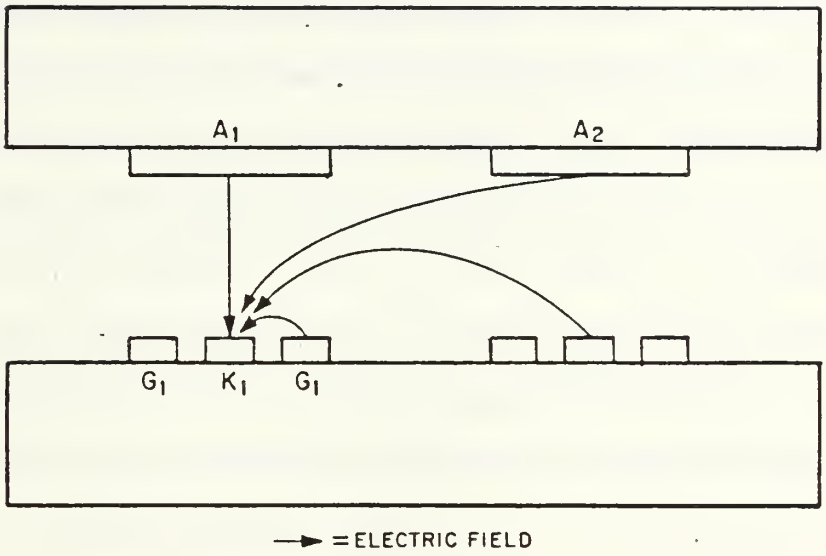

Figure 2-4. Undesireable Electrostatic Interactions

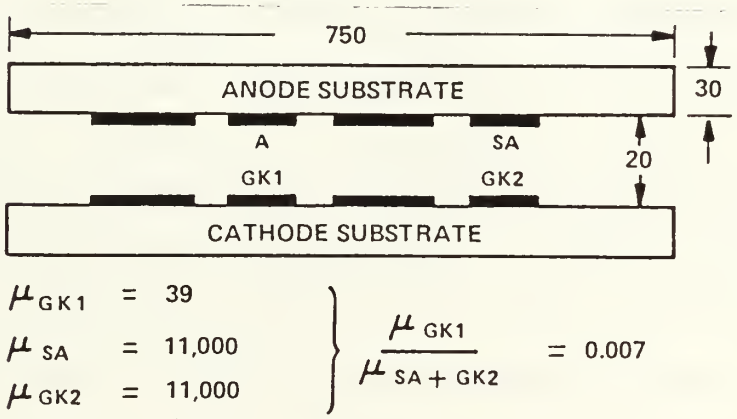

Figure 2-5. Sheild anode and grid cathode structure

of energy to be excited to a higher energy state but, remain bound to the parent atoms. If an electron absorbs sufficient energy to be completely removed from the parent atom, ionization has taken place. Ionization produces positive ions and free or unbound electrons. Ionization and excitation of lattice atoms may cause the atoms to give off photons.

An atom may give off a characteristic X-ray (photon) when one of its electrons has been removed (i.e. the atom has been ionized). X-rays will be emitted if a lower energy electron fills the empty energy state left due to ionization. The energy of the X-ray given off equals the difference in energy of the electrons involved in the transition .

$$h\nu = E_1 - E_2 \qquad (2.1)$$

An excited atom emits an X-ray when it transitions from an excited state to the normal ground state. Again, the energy of this transition is given by equation 2.1.

High energy electrons lose energy as they pass through material due to the emission of bremsstrahlung X-rays. Emission of bremsstrahlung is caused by the electric field of the atomic nucleus and the atomic electrons interacting with the high energy electrons bombarding the material. Bremsstrahlung is a smooth X-ray spectrum produced by the

electrons as they pass through material. As the electron slows down it gives up energy through radiation.

1. Photon Interaction in Material

Photons (gamma rays, X-rays and Bremsstrahlung X-rays) are slowed or stopped in material by three types of interactions; photoelectric collisions, compton effect and pair production. Reguardless of the manner in which the photons are produced they will interact with the lattice atoms of the material in one of the aforementioned manners. Once a photon is formed it's interaction process with a lattice atom is chiefly a function of the energy of the photon.

When the incident photon energy is less than 50 kev, the most probable photon interaction process is photoelectric collision. The probability of a photoelectric collision decreases with increasing photon energy. In photoelectric collisions the incident photon is completely absorbed by an atom and an electron is removed from one of the shells of the lattice atom. The free electron will have an energy E_e given:

$$E_e = h\nu - B_e \qquad (2.2)$$

where B_e is the binding energy of the electron. The removal of an inner electron (i.e. an electron not in the outer shell) will result in the emission of an X-ray [Ref. 5].

When a vacancy in one of the inner shells of an atom is filled by an electron from a higher energy state, a charecteristic X-ray is emitted. The energy of the X-ray is equal to the difference in the binding energy of the two electron states.

Auger electrons can also be produced by this effect but they will be ignored in this study due to their low energy.

In Compton collisions, the incident photon strikes an electron of a lattice atom but is not completely absorbed by the electron. The photon is scattered at a reduced energy by the collision. Part of the incident energy of the photon is absorbed by the electron and part of it is scattered as a lower energy photon. Compton scattering is most probable when the incident photon has an energy between .51-1.2 Mev. This energy is much greater than the binding energy of the atomic electrons, therefore the binding energy is not considered in the compton model [Ref. 6].

The maximum energy transferred to the electron is a function of the energy of the incident photon and the angle which it strikes the electron. The overall probability of Compton collision is proportional to the Z (atomic number) of the material and inversely proportional to the energy of the incident photon. The incident photons will cause the electrons to be ionized and forward scattered. When a large

number of compton collisions take place in a material, a net flux of electrons is produced in the material. These free electrons are called Compton electrons and constitute what is known as a Compton current [Ref. 7].

When the incident photons have an energy greater than 1.02 Mev pair production interaction becomes important. If the incident photon is completely absorbed by the lattice atom and a positron-electron pair equal in energy to the energy of the incident photon is formed, pair production has taken place. The positron-electron pair behave as free electrons from an ionized atom.

The high energy electrons bombarding any material will produce photons. The photons interacting in the material cause energy to be deposited. The energy deposited in the material is measured in rads (100 ergs/gm = 1 rad). The deposition of energy in material causes damage to the material and alters the normal characteristics of the material. Materials differ in their ability to absorb energy and maintain their normal behavior.

C. ELECTRON PRODUCTION OF FRENKEL PAIRS

The high energy electrons produced by the LINAC are focused into a tight beam of approximately one square centimeter when the beam strikes the TIC device. The beam is focused on the sapphire substrate inside the glass vacuum tube of the device.

The sapphire substrate and the metals on the substrate are highly ordered materials. The atoms in highly ordered materials form a orderly lattice structure. When one of the high energy electrons passes sufficiently close to the nucleus in the lattice it will penetrate the electron cloud surrounding the nucleus. Penetration of the electron cloud will cause the high energy electron to experience a deflection from the elctric field of the nucleus.

The magnitude of the screened electric field the bombarding electron will encounter is dependent upon the closest approach made with the nucleus of the atom in the lattice site. The interaction between the bombarding electron and the nucleus is known as coulomb scattering.

Coulomb scattering will cause the electron to transfer some of its energy to the atom of the lattice site. The bombarding electron can transfer a sufficient amount of energy to displace the nucleus of the atom in the lattice. When the nucleus of the displaced lattice atom moves from its normal lattice position, it may move to a new nonequilibrium position known as an interstitial position. The maximum amount of energy which can be transferred by an electron to the lattice atom is given by [Ref. 6]:

$$T_{max} = \frac{2(E+2mc^2)E}{Mc^2} \qquad (2.3)$$

where,

M ≡ mass of the lattice atom

m ≡ mass of an electron in units of mc

E ≡ bombarding electron energy

c ≡ speed of light

mc^2≡ rest mass energy (.511Mev)

Due to the long range interactions obtained with coulomb collisions, the average energy transferred to the lattice atoms is consideribly less than this maximum value [Ref. 8]. The average amount of energy transferred is given by:

$$T=T_d\left(\ln \frac{T_m}{E_d}-1+\pi\alpha\right) \qquad (2.4)$$

where,

T ≡ average energy transferred

E_d ≡ threshold energy to cause displacement in sapphire (50 ev for Al or 90 ev for O)

T_m≡ the maximum energy transfer possible

α ≡ Z/137

Z ≡ atomic number

If the elastic collision between the high energy electron bombarding the lattice atom transfers a certain threshold energy, E_d (50 ev for Al and 90 ev for O) the lattice atom will be displaced and moved to an interstitial position [Ref. 9]. If the energy transferred to the lattice atom is below E_d, the lattice atom will not be displaced. The displaced atom will leave behind a vacancy in the

lattice. The resulting vacany-interstitial pair is known as a frenkel defect. The process of the initial bombarding electron colliding with the lattice atom is known as the primary collision. The target atom of the lattice is called the primary knock-on.

The number of frenkel pairs produced per cubic centimeter can be computed as shown by Cahn [Ref. 10]. However, in computing the number of frenkel defects with this model numerous assumptions have been made. The assumptions are:

1) Step junction threshold energy is assumed (i.e., if E is greater than E_d there is displacement, if E is less than E_d no displacement).
2) Atom-atom collions are treated as hard sphere collisions.
3) The ordered arrangement of the atoms in the lattice structure is not considered.
4) Damage is considered homogeneous.
5) Annealing is not considered.
6) Glancing collisions are not considered even though an energy loss may be incurred.
7) Lattice atoms are considered at rest.
8) Long range effects from other atoms are not considered.
9) The number of replacements per primary are not

considered. The moving atom will replace the struck atom if the latter recieved energy greater than E_d and the former retains energy less than E_d.

10) There is no accounting for ionization losses. Kahn [Ref. 10] used the following formula to compute the number of frenkel pairs produced by bombarding electrons:

$$N_F = \Phi_e \sigma_d N_a \qquad (2.5)$$

where,

$\Phi_e \equiv$ electron fluence (electrons/cm^2)

$\sigma_d \equiv$ total cross-section due to primary and secondary displacements.

$N_a \equiv$ number of lattice atoms per cubic centimeter.

$$\sigma_d = \sigma_D \mu(t) \qquad (2.6)$$

where σ_D is given by [Refs. 10 and 11]:

$$\sigma_D = \pi\left(\frac{Ze^2}{mc^2}\right)^2\left(\frac{1}{\beta^2\Gamma^2}\right)\left[\left(\frac{T_m}{E_d}-1\right) - \beta^2 \ln\frac{T_m}{E_d} + \pi\alpha\beta\left\{2\left(\left(\frac{T_m}{E_1}\right)^{1/2}-1\right) - \ln\frac{T_m}{E_1}\right\}\right] \qquad (2.7)$$

where,

$\beta \equiv v/c$

$v \equiv$ speed of bombarding electron

$c \equiv$ speed of light

$\Gamma \equiv \sqrt{(1-\beta^2)}$

$\Gamma \equiv E/mc^2$

$$\mu(t) = \frac{BT\lambda}{E_d} \qquad (2.8)$$

B ≡ .5 (Kinchin and Pease constant)

$$\lambda = \frac{4M_1M_2}{(M_1+M_2)^2} \qquad (2.9)$$

$$N_d = \left(\frac{N_a}{A_t}\right) \text{[number of atoms/molecule]} \qquad (2.10)$$

where,

N_a≡ number of cattice atoms per cm^3

≡ 3.97 gm/cm^3 (density of Al_2O_3)

A_t≡ 82 gm/mole (atomic weight)

N_A≡ Avagodro's number (6.023×10^{23})

σ_d has included the effects of energy dependence and energy loss through ionization. As will be seen there is a strong dependence upon the stopping power of the material in computing the cross-section. Using equations 2.5-2.10 from above and the properties for sapphire the following predictions are made for the number of frenkel pairs.

N_F is the number of frenkel pairs produced per bombarding electron. This model predicts 1.0169 frenkel pairs per bombarding electron where, Φe is the electron fluence (electrons/cm^2).

Theoretical predictions for the number of frenkel pairs will exceed the actual values from observed experiments [Ref. 6]. The equations predict a value of four defects per cubic centimeter when bombarding gallium

arsenide and germanium with 1Mev electrons (assuming N_d = $5x10^{22}$ cm^{-3}). The experimental values for silicon were observed to be 0.26 per cm^{-3} by Wertheim [Ref. 6]. Ackerman and Graft report a value of 0.5 per cubic centimeter for gallium arsenide using 1 Mev electrons. Using 1.7 Mev electrons Cleveleand and Pacieses report values beteen 0.1 and 0.4 defects per cm^2 in gallium arsenide.

Not all of the frenekel defects produced by the electron bombardment are stable. At temperatures above 373 k the vacancies and interstitials are mobile in the crystal and unite with each other. Due to the high operating temperature of TIC devices (973-1123 K) only the permanent frenkel defects will remain.

Since the theory predicts 1.0169 frenkel defects per bombarding electron, it must be assumed that the total number of defects actually produced in the material is much less.

The production of frenkel defects alters the actual crystalline structure of the sapphire substrate. The damage caused to the sapphire alters the crystal's normal physical properties. Alteration of these properties could alter the performance of the TIC device.

D. STOPPING POWER

To get a measure of the amount of energy deposited by the electrons as they move through material we use the term

"stopping power". Stopping power is the amount of energy lost per unit length of path through the stopping material [Ref. 12].

For electrons it is customary to separate the total stopping power into two componants [Ref. 13]: (a) The collision stopping power is the average energy loss per unit path length due to inelastic coulomb collisions with bound atomic electrons of the medium resulting in ionization and excitation. (b) The radiative stopping power is the average energy loss per uint path length due to bremsstrahlung (radiation loss) in the electric field of the atomic nucleus and of the atomic electrons.

Stopping power is separated into two componants because the methods used for the evaluation of the two componants are quite different. The energy going into the ionization and excitation of lattice atoms is absorbed in the material close to the track of the bombarding electron. The energy lost by the bombarding electrons due to bremsstrahlung travels far from the electron track before being absorbed. In "thin sample" (the sapphire substrate is considered a thin sample) the energy lost due to bremsstrahlung is not deposited in the material.

Radiative and collision stopping power both slow electrons. The energy due to radiative stopping power is deposited far from the electron track. Collision stopping power is the mechanisum which creates ionization and causes

energy to be deposited in the material. Collision stopping power is the mechanisum responsible for energy deposition in the TIC device used for this thesis. The total amount of energy deposited in the material (measured in Rads Si) required to affect the TIC devices perfomance will be the focus of this thesis.

The formulas for stopping power used in this section come from Beth's theory and refinements to that theory. The electron mass collision stopping power is given by the formula developed by Rohrlich, Carlson and Ueling [Ref. 13]:

$$\frac{1}{\rho}\frac{dE}{dX} = \frac{2\pi N r_e^2 mc^2 Z}{\beta^2 A}\left[\ln\left(\frac{T}{I}\right)^2 + \ln\left(1+\frac{\tau}{2}\right) + F(\tau) - \delta\right] \qquad (2.11)$$

where,

$$F(\tau) = \left(1-\beta^2\right)\left[1 + \frac{\tau^2}{8} - \left(2\tau+1\right)\ln 2\right] \qquad (2.12)$$

the quantity;

$$.5\left[\ln\left(\frac{T}{I}\right)^2 + \ln\left(1+\frac{\tau}{2}\right) + F(\tau) - \delta\right] \qquad (2.13)$$

is the stopping power per atomic electron [Ref. 12].

N ≡ Avagodro's number (6.023×10^{23})

Z ≡ atomic number of the target atoms

I ≡ mean excitation energy

mc^2 ≡ electron rest energy

β ≡ velocity of high speed electron/speed of light

$\tau \equiv T/mc^2$ kinetic energy of incident electron per rest mass.

$r_o \equiv$ classical rest energy

$A \equiv$ atomic weight of the target atoms

The collision stopping power for electrons in Al_2O_3 is 1.75 Mev cm^2/gm for 30 Mev electrons and 1.851 Mev cm^2/gm for 100 Mev electrons [Ref. 9].

The mass radiative stopping power can be expressed as [Ref. 12]:

$$\frac{1}{\varrho}\frac{dE}{dX} = \frac{N\alpha r_o^2 Z^2}{A}\Phi_{rr}\left(1 + \frac{\Phi e}{Z\Phi_{rr}}\right) \qquad (2.14)$$

where,

$N \equiv$ Avagodro's number (6.023×10^{23})

$Z \equiv$ atomic number of the target atoms

$r_o \equiv$ classical electron radius

$\alpha \equiv$ fine structure constant ($Z/137$)

$E \equiv T + mc^2$ total energy of the electron

$\Phi_{rr} \equiv$ scaled radiative energy cross-section for electron-nucleus interaction

$\Phi e \equiv$ scaled radiative energy-loss cross-section for electron-electron interaction

$A \equiv$ atomic weight of the target atoms

The mass radiative stopping power depends implicitly upon the bremsstrahlung cross-section. The bremsstrahlung cross-section is the probability of the emission of a photon due to interaction of the electron with the screened coulomb

field of the atomic nucleus, and the corresponding probability of the emission of a photon due to interaction with one of the atomic electrons [Ref 12].

The range of an electron is the average length of path the electron travels until it is stopped by the medium due to energy loss [Ref. 11]. The electron is assumed to lose energy continuiously along its path. Range is given in term of (gm/cm^2). When the range is divided by the density, the average distance an electron will travel in the medium can be computed.

Dose is the total energy deposited in the material by the interacting radiation. Dose is measured in rads and must be specified for the material. The front surface dose (for a thin sample) is expressed by the following formula [Ref. 13]:

$$R = 1.6 \times 10^{-8} \Phi e \frac{1}{\rho} \frac{dE}{dX} \quad \text{(rad material)} \qquad (2.15)$$

The dimensions of the substrate constitute a thin sample and therefore equation 2.15 will be used to compute the dose measured in rads Si.

III. EXPERIMENT

A. DEVICE FABRICATION

Figure 3-1 shows a TIC triode package. The sapphire substrates are 2 cm (approx .75 in) in diameter and 30 mil thick. The integrated circuits are manufactured on the substrate using photolithographic and fabrication techniques developed for the manufacture of typical integrated circuits. Figure 3-2 shows the grid and cathode circuitry on the sapphire substrate. Figure 3-3 shows the anode circuitry on the sapphire substrate.

The circuit side of a device is made up by laying down thin films of metal on the sapphire substrate. Figure 3-4 shows the procedure used in laying down the tungsten, molybdenum and titanium of the integrated circuit. The pattern of the circuit is defined using a plasma etch procedure. The titanium and molybdenum are removed from the cathode using a sputter etch technique in argon gas. The final process of delineating the circuit is accomplished by adding a photoresist-cathode coating. The coating is a combination of standard vacuum tube barium-stronium-calcium carbonate powder and negative photoresist. The anode is layed down in a similar manner.

A heater element is layed down on the reverse sides of both substrates to ensure a uniform temperature (Figure

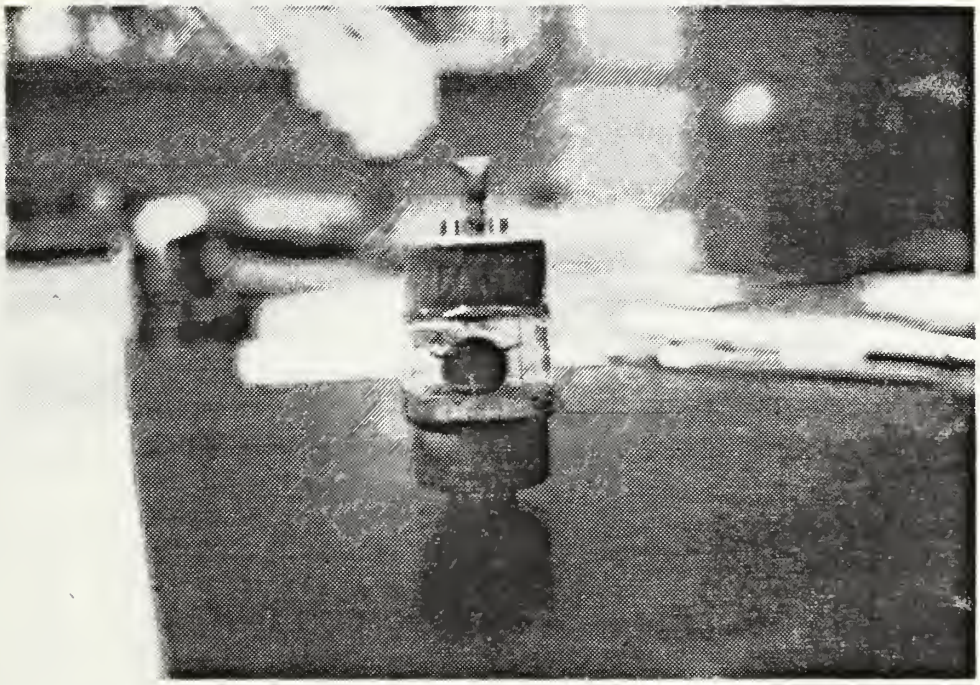

Figure 3-1. Triode package used for the irradiation studies.

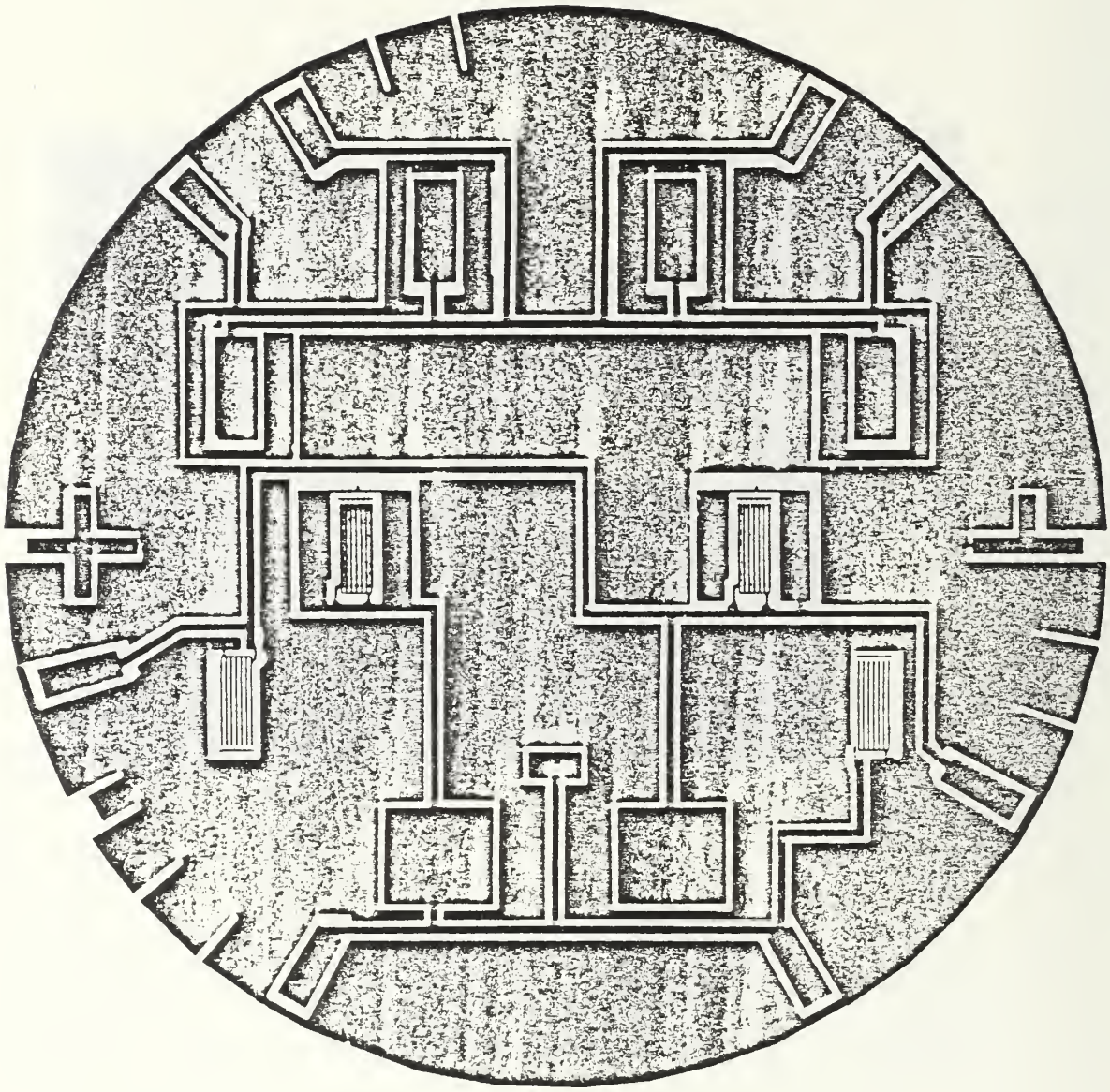

Figure 3-2. The circuitry of the grid and cathode on the substrate.

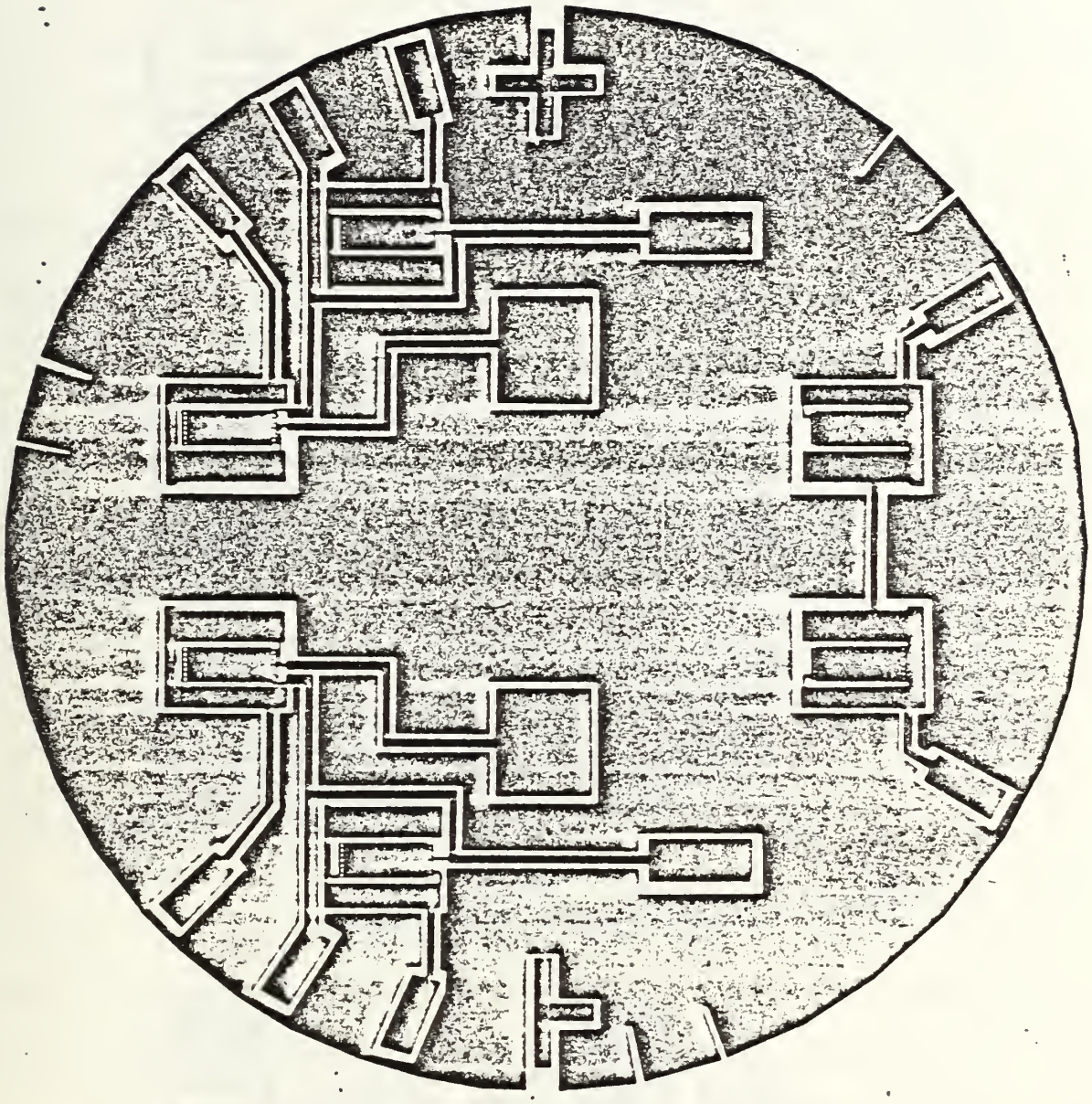

Figure 3-3. The circuitry of the anode on the substrate

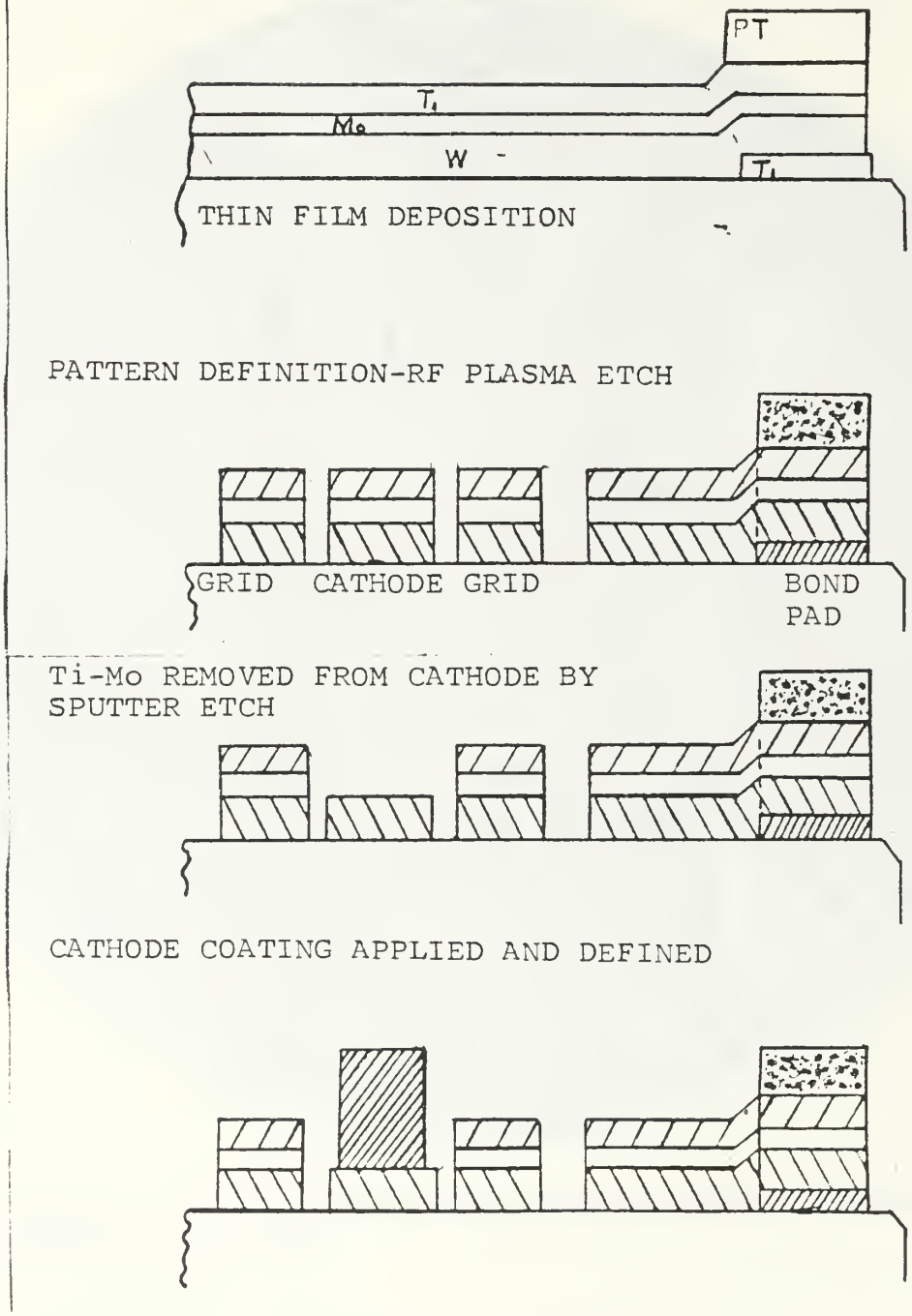

Figure 3-4. Fabrication procedure

3-5). The heater is required for proper device operation. The heater power requirement for the TIC is 15 watts per .75 in. diameter substrate pair when heated to 1023 K.

Figure 2-2 shows a representation of one integrated circuit. The typical TIC triode is made with seven 1.5 mil-wide cathode stripes per device, with 1.0 mil-wide grid strips between cathodes.

The current assembly technique for the substrates uses three 40 X 50 mil platinum straps bonded to each substrate at 120 degree intervals. The substrates are aligned with respect to each other by viewing the "cross and tee" alignment keys shown on the circuit patterns (Figure 3-6). The heater windows permit viewing the alignment keys (Figure 3-5). Nickel shims welded to the straps govern the substrate seperation.

The TIC device is pumped for 72 hours to obtain the proper vacuum inside the tube. This is followed by a pre-activation bakeout at 673 K for 15 hours. The substrates are heated to 1123 K to complete the activation process.

The lifetime of TIC devices manufactured using the sputter etch technique is decreased due to the argon gas. The argon molecules attach themselves to the sapphire substrate. When the device is activated the argon atoms detach themselves from the substrate, become ionized and slowly poison the cathode. The process of poisoning the

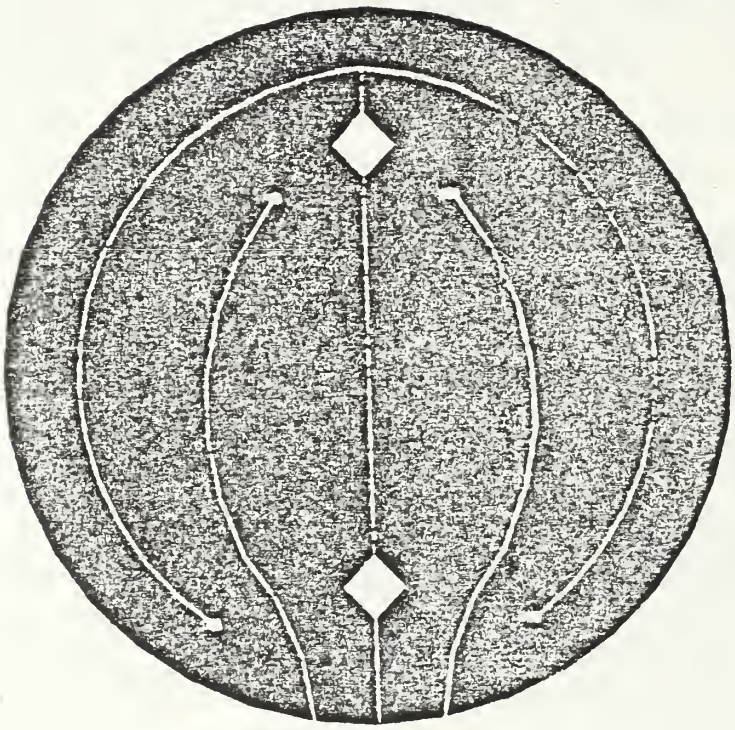

Figure 3-5. Heater element of the TIC device The diamond shaped holes are for viewing the cross and tee of the circuits.

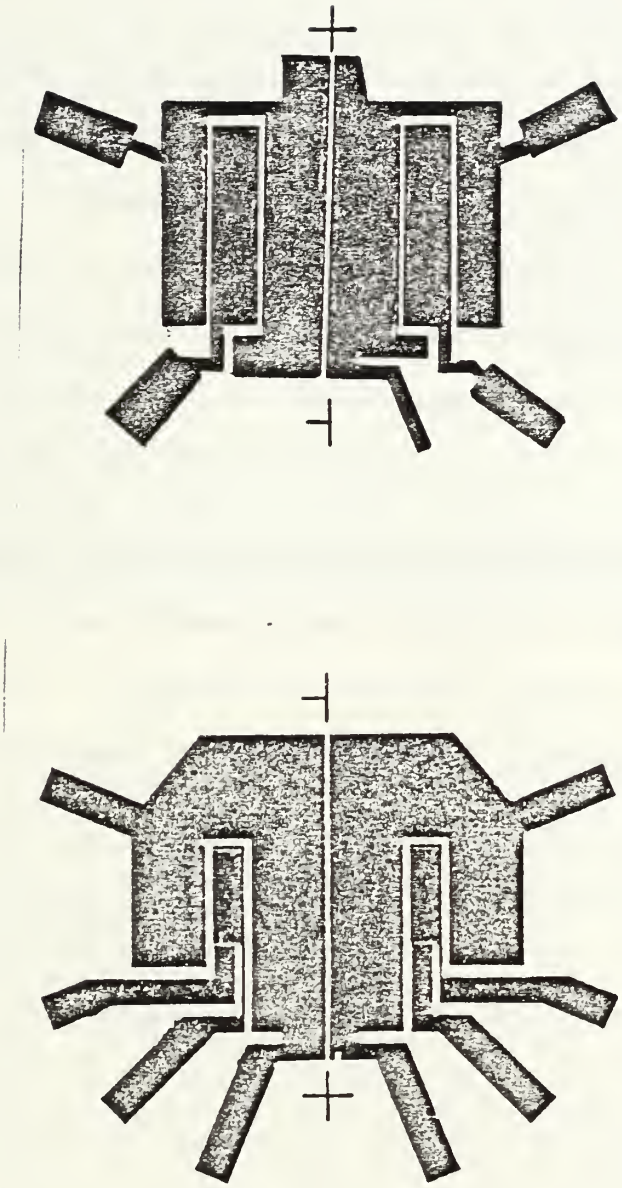

Figure 3-6. Cross and tee arrangement

cathode eventually causes the cathode to cease emitting electrons [Ref. 4].

A change in the etching technique will eliminate the problem of cathode poisoning. A chemical etch process is currently being developed at Los Alamos National Laboratory to replace the sputter etch technique using argon gas. The change in the etching process will eliminate the tendency for TIC devices to self-destruct.

B. NPS LINAC

The Naval Postgraduate School Linear Accelerator (LINAC) is a disk-loaded circular waveguide, thirty feet long consisting of three ten-foot sections. Each ten-foot subsection is powered by a klystron amplifier used to accelerate electrons from 15 -100 Mev. The LINAC operates at 60 pulses per second with a microsecond pulse duration. The relativistic electrons are focused on a target using deflection and focusing magnets. A target can be placed either inside the target chamber (held at a vacuum of about one torr) or just outside the the target chamber. When the target is placed outside the target chamber it is placed against the target chamber window (the target chamber window is a thin aluminum plate).

The electron fluence (electrons/cm^2) is measured using a Secondary Emission Monitor (SEM) located inside the target chamber. The electrons which impact the SEM charge a

capacitor. The voltage developed across the capacitor is measured by a voltage integrator. The voltage charge relationship is given using the following equation:

$$Q_{SEM} = CV \tag{3.1}$$

where,

Q_{SEM} ≡ the charge on the capacator of the SEM

C ≡ the capacitance

V ≡ the accumulated voltage

The total number of electrons that have passed through the SEM is computed using the following equation:

$$N = Q_{BM}/q \tag{3.2}$$

where,

N ≡ the total number of electrons

Q_{BM} ≡ the beam charge

q ≡ electron charge

Previous radiation studies using the NPS LINAC have calibrated the large external SEM with the use of a faraday cup [Ref 14].

Studies of the NPS LINAC have shown the large outside SEM to be 6% efficient in collecting electrons when compared to the faraday cup. The faraday cup has since been removed and the large SEM is the standard. The small internal SEM used for the calculations in this thesis has been calibrated against the large SEM. The small SEM is 2.6% efficient in

collecting electrons, so that Q_{m} = .026 Q_{B} Using this information and equation 3.2 the total number of electrons is given by:

$$N = CV/.026q \qquad (3.3)$$

The fluence (Φ) is computed by dividing both sides of equation 3.3 by the area of the beam (for further explaination see section IV. Data and Results):

$$\Phi = CV/.026Aq \qquad (3.4)$$

$\Phi \equiv$ the fluence used in this thesis computed using equation 3.4.

C. EXPERIMENTAL PROCEDURE

1. Pre-irradiation Measurements

The TIC triode was placed on the test stand as pictured in figures 3-7 and 3-8 . It was activated to the normal operating parameters by heating the substrates to 1023 K using 1.21 amps.. The temperature of the substrate was measured using an optical pyrometer. The TIC device was allowed an 8 hour warm-up period before recording the v-i characteristics (hereafter referred to as the baseline characteristics). The cathode, anode and grid of the device were used as inputs for a textronix 576 curve tracer. Figures 3-9 and 3-10 show the pre-irradiation v-i charecteristics of this TIC device. This device exhibits

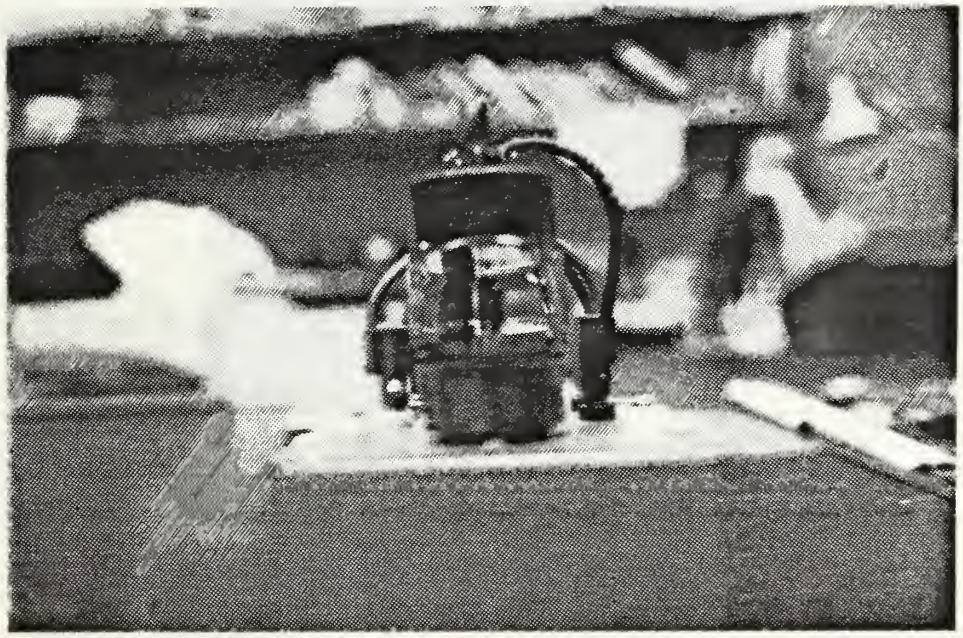

Figure 3-7. TIC device on curve tracer stand

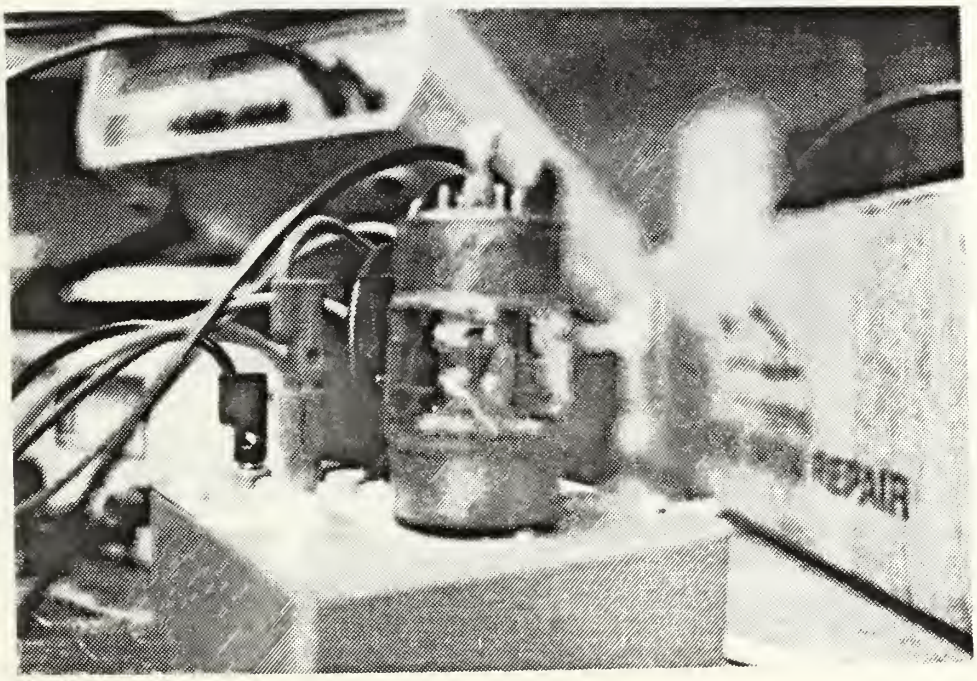

Figure 3-8. TIC device on test stand and banana plugs used to connect the device to curve tracer

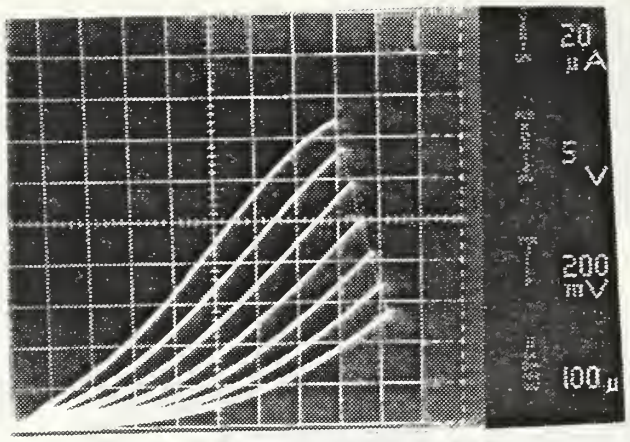

Figure 3-9. v-i characteristics prior to irradiation

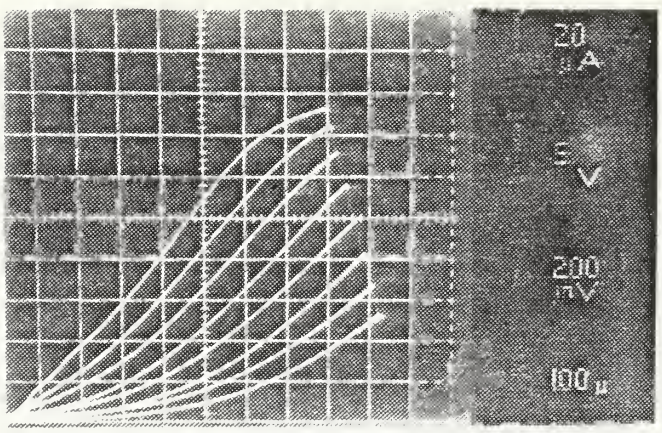

Figure 3-10. Pre-irradiation v-i characteristics

Figures 3-9 and 3-10 are known as the baseline characteristics.

the typical exponential curve expected from a vacuum triode [Ref. 4].

2. Pre-irradiation Procedure

The TIC triode was placed on the test fixture as shown in Figure 3-11 during the irradiation portion of the experiment. The stand and device were placed inside the target room just outside the target chamber as close as possible to the target chamber window. The device was activated to the normal operating parameter of 1023 K.

A target made of phospherous on an aluminum screen was set upon the stand (see Figure 3-12). The target area was of equal height to the substrate disks of the TIC. The electron beam of the LINAC was focused and aligned on the phospherous target. The electron beam appears as a very bright area on the phosperous target.

The alignment and focusing of the beam on the target was monitored through a video camera. The camera located in the target room relayed the video of the beam on the target to the control room. Using the focusing and alignment magnets the electron beam is centerd on the target and adjusted until the beam area is one square centimeter.

A circle is drawn on the video monitor enclosing the beam as it appears on the phospherous target. The beam is then shut off and the TIC device is aligned so the one square centimeter area of the beam will be centered on the substrate disks of the TIC device. The test stand and TIC

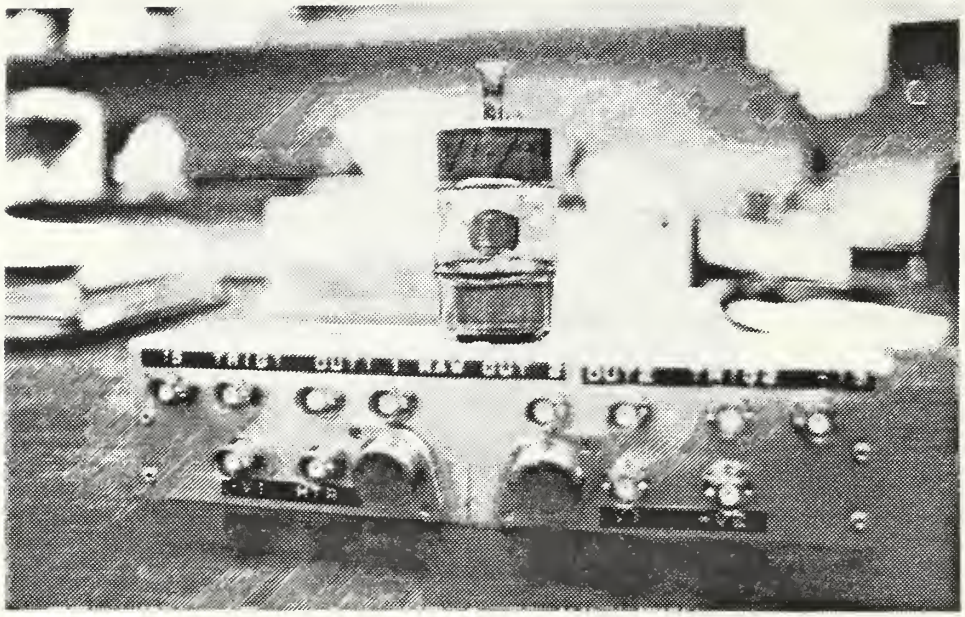

Figure 3-11. TIC device on test stand

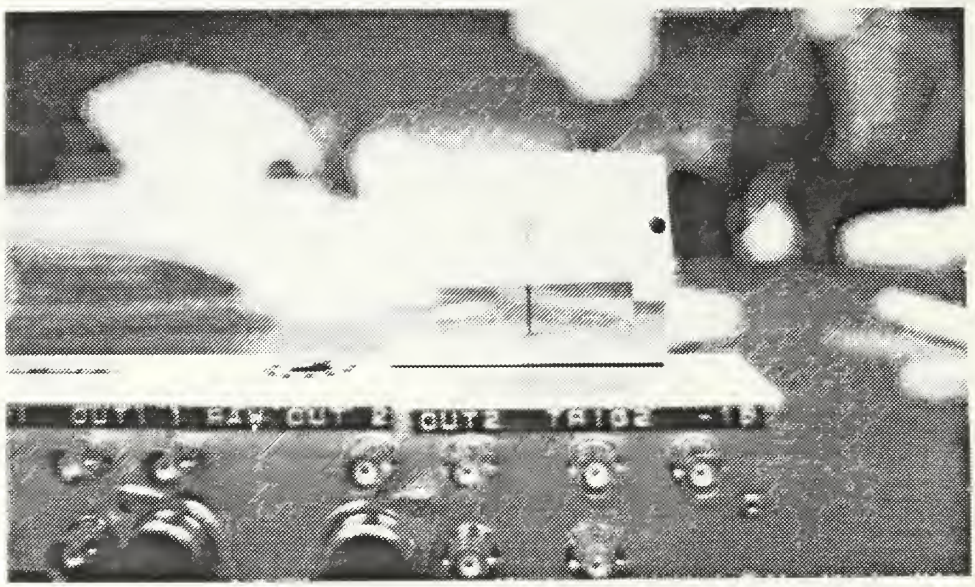

Figure 3-12. Target used to focus electron beam

device (see Figure 3-11) placed as close to the target chamber window as possible (approximately 5 mm from the window).

Figure 3-13 depicts the circuit used for the triode radiation tests. The 50 volt power supply provides 50 volts across the cathode and anode. The 50 volts was also used as the input to an oscilloscope after passing through a 250 K Ω resistor. Irradiation of the TIC triode commenced after the circuit was activated.

3. Test Procedure

The procedure for the radiation test was as follows:

a. Place the device on the test stand as in Figure 3-11 and heat it to normal operating parameters.

b. Irradiate the TIC device using the desired electron beam energy of 30 or 100 Mev for a specified amount of time.

c. Monitor the irradiation of the device by viewing and photographing the signal received by the oscilloscope from the TIC triode.

d. After irradiating the device for a specified period of time the electron beam is secured. The device is allowed to cool to ambient temperature.

e. The device is placed on the test stand as in Figures 3-7 and 3-8. The post irradiation v-i charecteristics from the curve tracer are photographed and compared with the baseline characteristics.

Steps a-e were repeated five times. The first irradiation of the device used 30 Mev electrons, while 100 Mev electrons were used for the next four experimental runs.

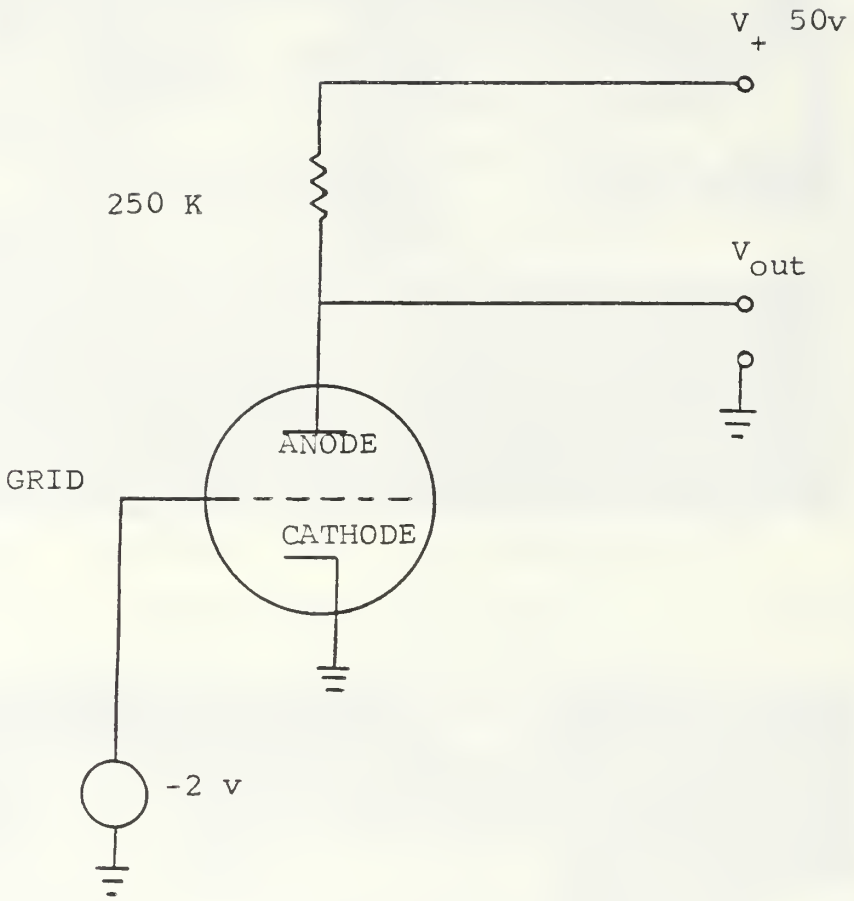

Figure 3-13. Representation of the wiring circuit

The length of time the device was exposed to irradiation was increased during each subsequent experimental run.

A problem with 120 volt a.c. noise was discovered after the second experimental run (for further information see discusion of data and results). To assist in identifing actual changes in the operating charecteristics of the device, a square wave generator was used. The input and output of the square wave through the TIC device was observed and photographed via the oscilloscope. The square wave generator was used before and after irradiation during the third, fourth and fifth experimental runs.

IV. DATA AND RESULTS

A. BASELINE DATA

Figures 3-9 and 3-10 are photographs of typical v-i charecteristics of the TIC device prior to irradiation. All post-irradiation v-i charecteristics will be compared with these baseline photographs to access changes in perfromance charecteristics. The drop in electron emission by the cathode will be monitored by watching the decrease in the height of the emission lines (measured up the vertical axis). A decrease in the height of the emission lines is expected as the argon poisons the cathode. A decrease in emission is not an indication of radiation damage, but, a consequence of manufacturing technique.

B. IRRADIATION

During irradiation of the TIC device charge builds up and dissipates in the device. Figures 4-1 and 4-2 are typical of the charge build up and dissipation. All experimental runs showed this behavior and it is more prominent when using 100 Mev electrons.

The first experimentsl run was completed using 30 Mev elctrons for 56 minutes. The four succeeding runs were completed using 100 Mev electrons. Table 4-1

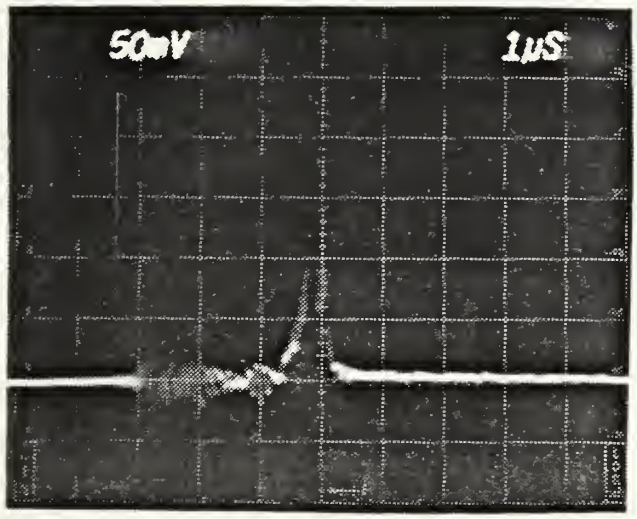

Figure 4-1. Charge build-up

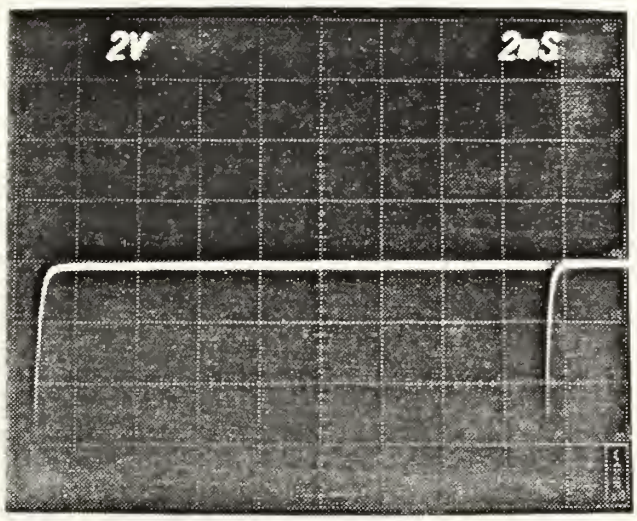

Figure 4-2. Charge build-up

below gives the time of irradiation for each experimental run.

TABLE 4-1 EXPERIMENTAL RUN AND TIME OF IRRADIATION

Experimental Run	Time of Irradiation
Two	1hr. 6 min.
Three	1hr. 10 min.
Four	1hr. 28 min.
Five	2hr. 10 min.

C. DOSE COMPUTATION

Equation 4.1 gives the fluence when the capacatance (C), voltage (V), area (A), and the charge (q) are known. The costant .026 is due to the internal SEM used during all of the experimental runs.

$$\Phi = CV/.026qA \qquad (4.1)$$

One rad(R) is equal to 100 ergs/gm energy deposited in the material. One rad Al_2O_3 is not the same as one rad Si but a conversion factor can be used to equate the two materials [Ref. 14] . The number of rads ($R_{Al_2O_3}$) in Al_2O_3 is computed using equation 4.2:

$$R_{Al_2O_3} = 1.68 \times 10^{-8} \Phi * \left[\frac{1}{\rho}\frac{dE}{dX}\right] \qquad (4.2)$$

where $R_{Al_2O_3}$ is in rads Al_2O_3

This is a variation of Rudi's equation for dose [Ref. 14]. $\frac{1}{\rho}\frac{dE}{dX}$ is the stopping power. It is a function of the

material and the energy of the bombarding electrons. The value of this function is 1.75 Mev cm^2/gm for 30 Mev elctrons and 1.851 Mev cm^2/gm for 100 Mev electrons.

For the first experimental run the following values were used:

$C = 1 \times 10^{-6}$ f

$q = 1.602 \times 10^{-19}$ coul.

V = 11 volts

.026 is the efficiency factor for the internal SEM

$A = 1\ cm^2$

$\left[\frac{1}{\varrho}\frac{dE}{dX}\right] = 1.75$ Mev cm^2/gm

$$\Phi = 2.64 \times 10^{15} \text{ [electrons/cm}^2\text{]} \quad (4.3)$$

$$R_{,,} = 1.68 \times 10^{-8} * 2.64 \times 10^{15} * 1.75 \text{ [rad } Al_2O_3\text{]} \quad (4.4)$$

$$R_{,,} = 7.39 \times 10^{7} \text{ [rad } Al_2O_3\text{]} \quad (4.5)$$

To compute dose in terms of [rad Si] the the stopping power of silicon is divided by the stopping power of sapphire. This conversion factor is multiplied by the dose in Al_2O_3.

$$R_{,,} * 1.809/1.75 = 1.034 * R \text{ [rad Si]} \quad (4.6)$$

$$R = 1.034 * 7.39 \times 10^{7} \quad (4.7)$$

$$R = 7.64 \times 10^{7} \text{ [rad Si]} \quad (4.8)$$

The dose for the other four runs was computed using the same equations. When the bombarding electrons have an energy of 100 Mev:

$$\left[\frac{1}{\varrho}\frac{dE}{dX}\right] = 1.851 \text{ Mev cm}^2/\text{gm } (Al_2O_3) \quad (4.9)$$

$$\left[\frac{1}{\varrho}\frac{dE}{dX}\right] = 1.918 \text{ Mev cm}^2/\text{gm (Si)} \quad (4.10)$$

1.034 is the factor to convert dose ($R_{Al_2O_3}$) in rads Al_2O_3 to dose (R) in rads Si.

During the last four experimental runs:

$q = 1.602 \times 10^{-19}$ coul.

$A = 1 \text{ cm}^2$

$C = 1 \times 10^{-6}$ f

.026 due to the internal SEM

Table 4-2 below give the summation of the results of experimental runs two through five.

TABLE 4-2 SUMMATION OF DOSE (R rad Si) FOR EXPERIMENTAL RUNS TWO THROUGH FIVE.

Experimental Run	Voltage of SEM	R [rad Si]
Two	20.1	1.48×10^{6}
Three	60	4.42×10^{6}
Four	66	4.862×10^{6}
Five	90	6.629×10^{6}

$$R_{total} = R_1 + R_2 + R_3 + R_4 + R_5 \qquad (4.11)$$

$$R_{total} = 1.8155 \times 10^7 \text{ [rad Si]}$$

R_{total} is the total radiation to which the TIC device was exposed over a period of five experimental runs.

D. RESULTS OF IRRADIATION

Figure 4-3 is a baseline photograph of the v-i characteristics of the TIC device. Figure 4-4 is a photograph of the v-i charecteristics of the TIC device after exposure to 1.8155×10^7 [rad Si]. Although the emission is down due to cathode poisoning the device is exhibiting no characteristics which would indicate damage due to radiation [Ref. 4].

Figure 4-5 and 4-6 show the square wave input before and after irradiation of experimental run three. There is no reduction in the TIC device's ability to transmit the square wave input.

Figure 4-7 is a photograph taken after experimental run three. The strange humps approximately one half way along the emission lines were thought to be due to radiation damage. After consulting with Los Alamos National Laboratoty an attempt was made to filter out any noise in the 120 volt a.c. circuit. It was determined that the cause of the humps was noise feeding through the 120 volt a.c. circuit into the curve tracer. A SOLA inverter-rectifier

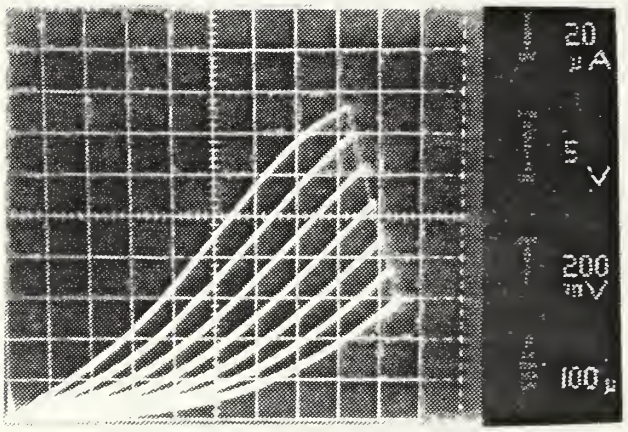

Figure 4-3. Pre-irradiation v-i characteristics

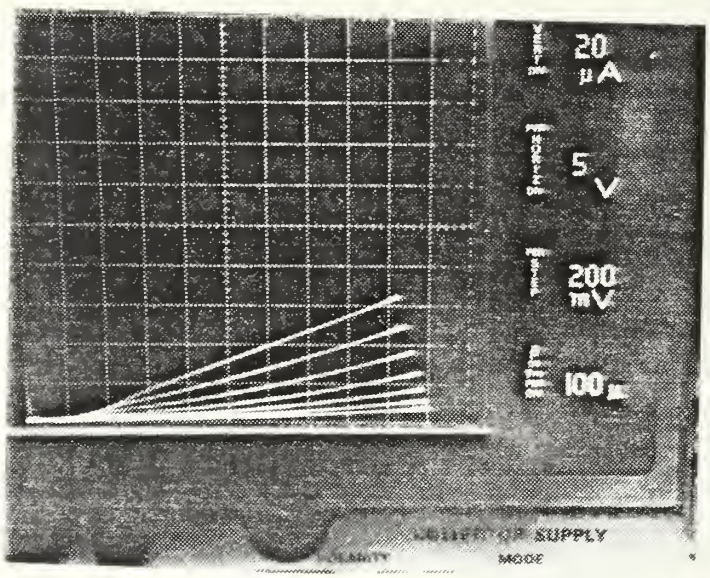

Figure 4-4. Post-irradiation v-i characteristics

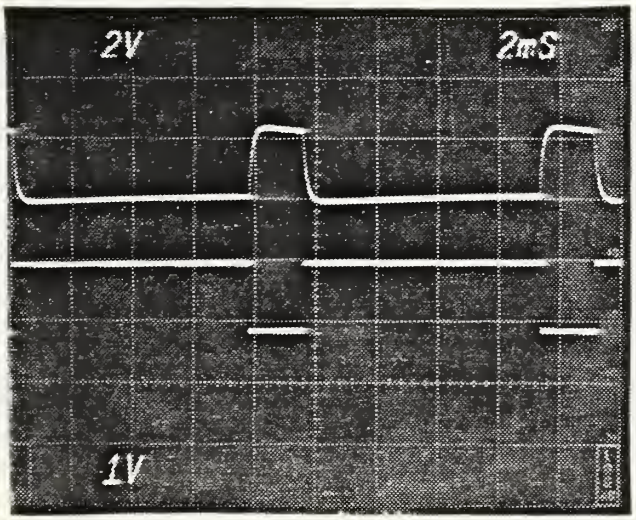

Figure 4-5. Square wave input prior to experimental run three

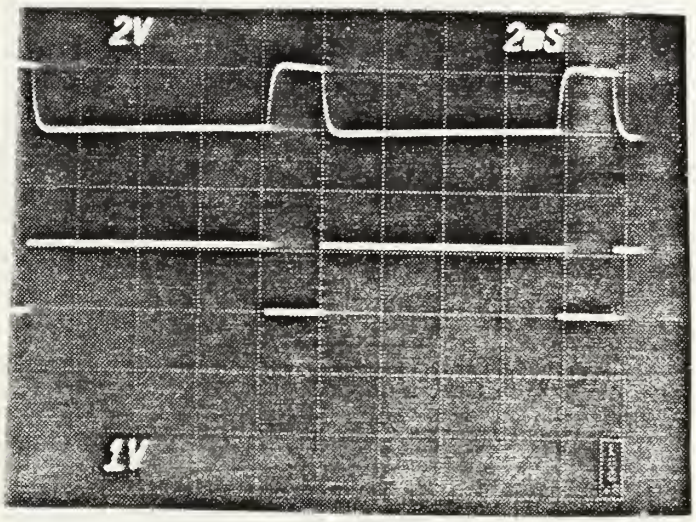

Figure 4-6. Square wave input after experimental run four

was used to filter out the noise. Figure 4-8 shows a photograph taken after experimental run three using the SOLA. Then the strange humps have disappeared and the device exhibited normal behavior.

Figure 4-9 shows the TIC device's ability to transmit a square wave prior to experimental run five. Figure 4.10 shows the TIC device transmitting a square wave after experimental run five. The TIC device's performance is relatively unaffected even by this large dose of radiation.

E. STRUCTURAL FAILURE OF THE DEVICE

Continued radiation studies on this device could not be conducted because a weld on one of the bond straps failed. The weld which holds the bond strap to the support pin failed (see figure 1-1). The bond straps and shims are used to maintain the alignment and spacing between the integrated circuits.

The broken weld allowed the critical spacing between the substrates to be greater than normal. When the substrates changed position the integrated circuits became misaligned and the device would no longer fuction properly.

Figures 4-11 and 4-12 show the response of the device with the broken weld. The respose of the device when connected to the Textronix 576 curve tracer shows that the device will no longer function properly.

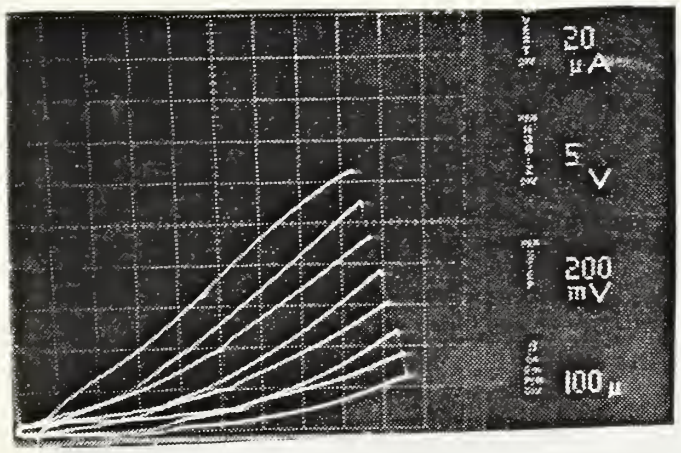

Figure 4-7. v-i characteristics without the SOLA inverter rectifier

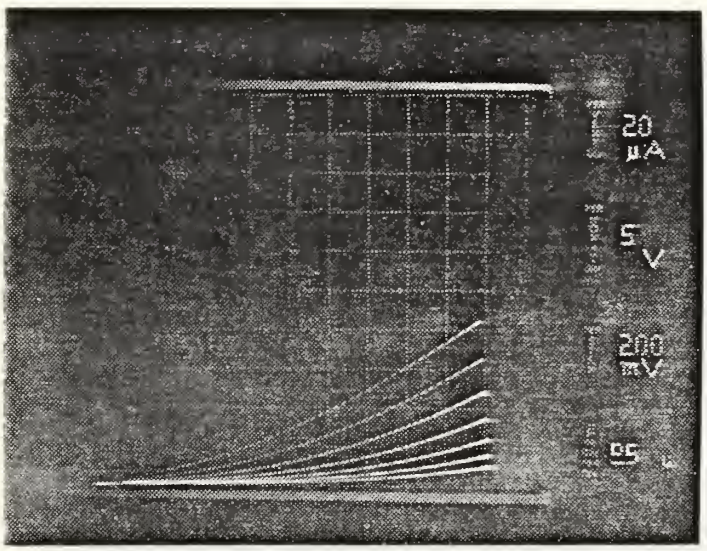

Figure 4-8 v-i characteristics using the SOLA inverter rectifier

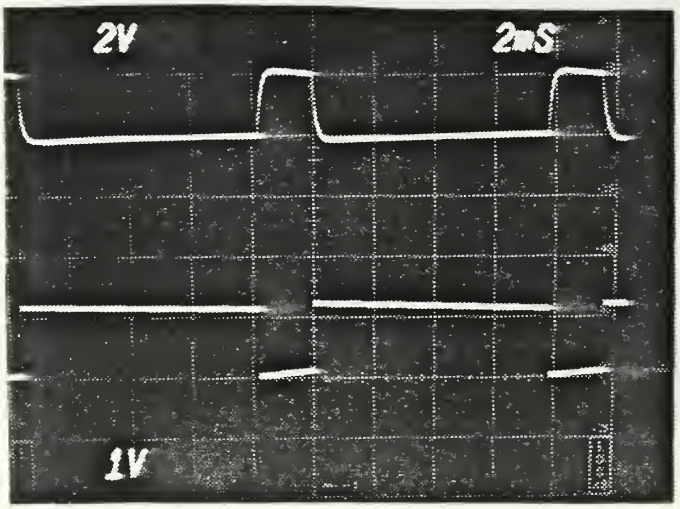

Figure 4-9. Square wave input prior to experimental run five

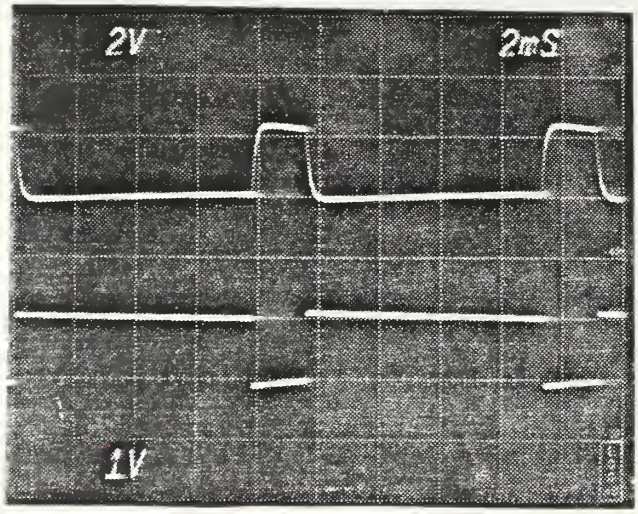

Figure 4-10. Square wave input after experimental run five

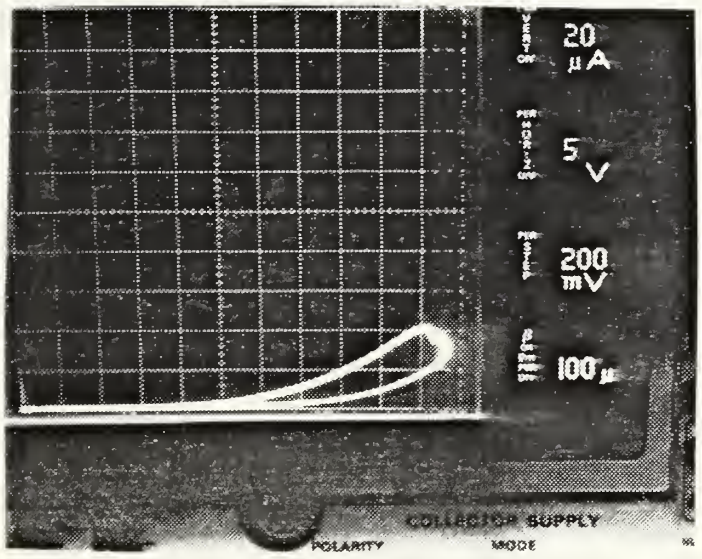

Figure 4-11. v-i characteristics of TIC with broken bond strap

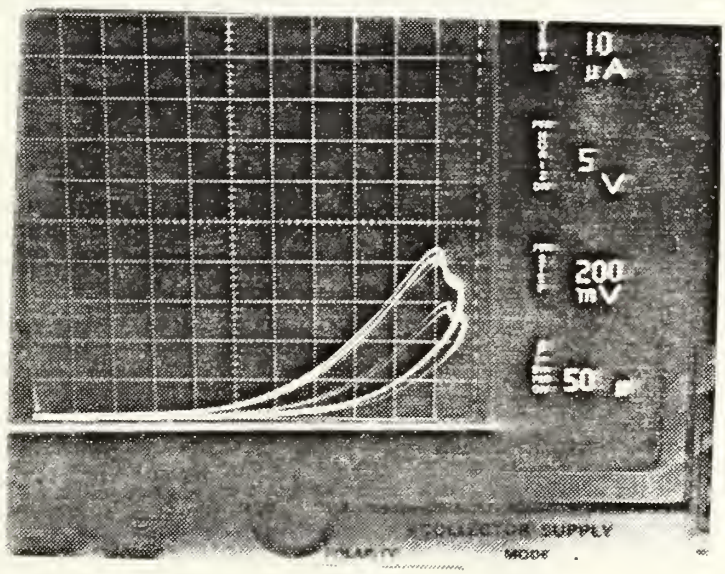

Figure 4-12. Response of TIC to a change in current with broken bond strap

The broken weld of the bond strap was a structural failure. There is no reason to believe or assume that the broken weld was caused by radiation damage.

F. PREVIOUS RADIATION STUDIES

Previous studies have been performed on TIC triode devices. The earliest tests were conducted at the University of Arizonia (U. of A.) in July of 1979. The U. of A. tests were perormed using a TRIGA reactor capable of 100 kw continuous and 750 mw pulsed operation. The triode device was continuously monitored for changes in characteristics. When the reactor was pulsed to 750 Mw the TIC triode characteristics showed an istantaneous shift during the pulse. After the pulse the recovery was almost immediate. The total dose (2.5×10^{8} rad Si) produced no effect on the device characteristics.

This was the only test run for the purpose of total dose. All other tests were conducted to establish the dose rate response rate of the devices. None of the tests produced any long term negative effects on the TIC triodes.

G. RADIATION HARDNESS OF TYPICAL MICROCIRCUITS

Semiconductor integrated circuits are classified by thechnology. The different microcircuit technologies and their respective hardness to total dose (rad Si) radiation damage are shown by figure 4-13. [Refs. 16,17,and 18] The relative hardness of the different

technologies varies widely. The broad range of failure levels makes comparisons, even within the same family trecherous [Ref.19]. TIC devices have withstood total dose levels two orders of magnatude greater than any other integrated circuitry and continue to function normally.

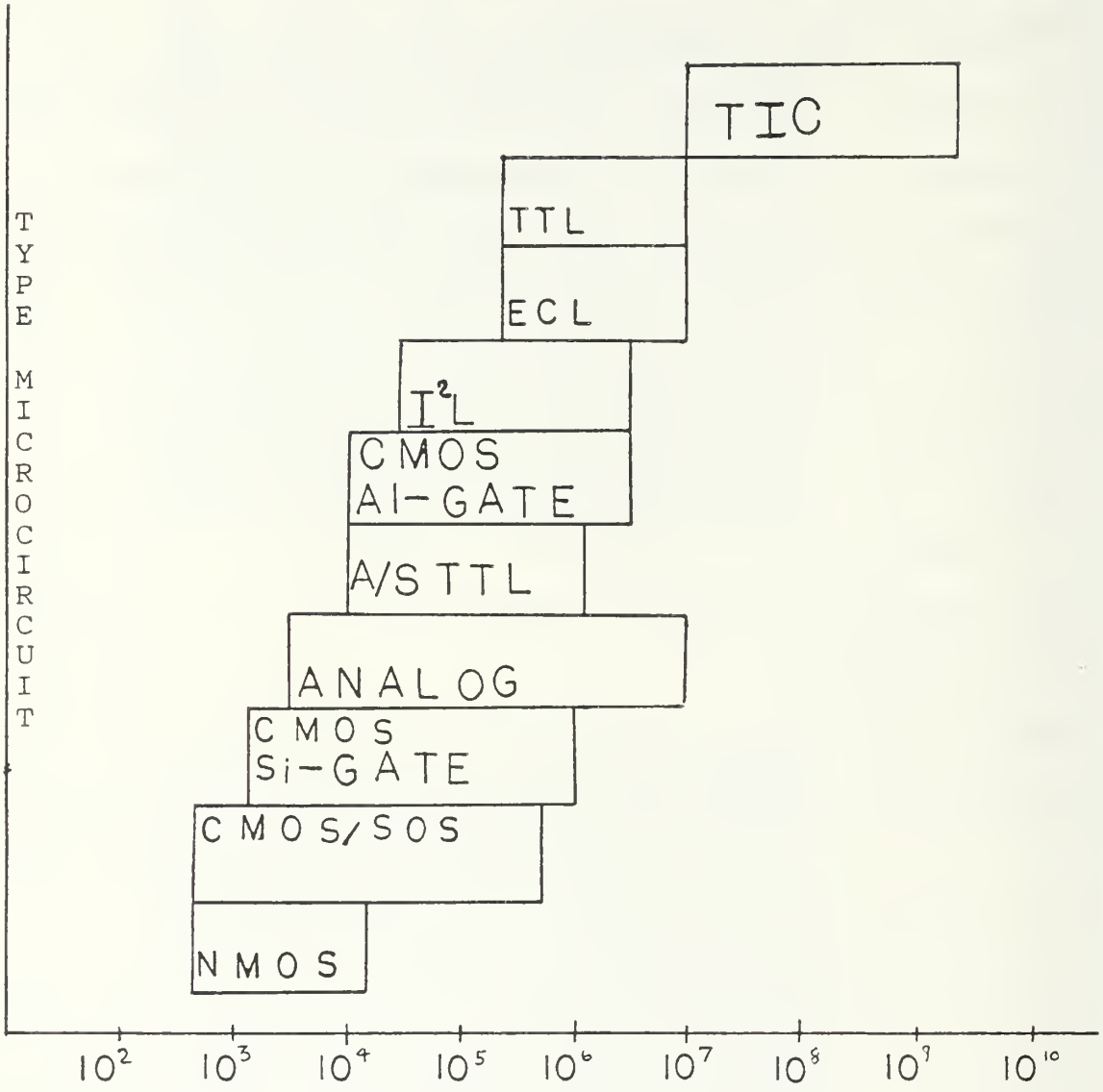

Figure 4-13. Relative hardness of microcircuits

V. CONCLUSIONS

A. RESULTS OF RADIATION STUDIES

TIC triode devices have proven to be very "hard" to radiation damage. Previous studies have shown bombarding neutrons have no long term effect on TIC device operating characteristics. The previous study tested TIC devices to a total dose (R) of 2.5×10^{8} rad Si [Ref. 1].

The low radiation hardness of present day microcircuits makes them vulnerable to failure. A total dose of 10^{4} rad Si is fatal to the hardest of todays integrated circuits. The TIC triode used in this experimental study was subjected to a total dose (R_{total}) of 1.8155×10^{7} rad Si. The device continued to function as expected showing no ill effects due to radiation damage. The results of this experimental study show that TIC integrated circuits are at least two orders of magnatude more resistant to radiation damage.

The electron emission of the device dropped off as expected. The decrease in electron emission was not due to radiation damage. The sputter etch process used to fabricate the integrated circuitry causes cathode poisoning [Ref. 4] . New device manufacturing techniques soon to be introduced will eliminate this problem.

Although the TIC device did eventually fail, the failure was not due to radiation damage. The structural failure of a weld cannot be attributed to radiation damage of the material. However, this failure did cause the termination of experiments before radiation failure could be determined. The operating circuitry of the device did not fail. TIC devices represent the forefront of a new technology. Manufacturing and design problems are to be expected from any new technology. The next generation technology of TIC devices will eliminate these problems.

None of todays modern integrated circuit devices can withstand the total dose to which this TIC device was subjected and continue to function. The fact that TIC devices require no additional sheilding to operate in such a hostile radiation environment will be the impetus for further developement.

Thus, the present electron radiation experiments and the earlier neutron irradiations demonstrate that TIC devices can operate in very high radiation environments with no degregation in performance. TIC devices have continued to function normally after a total dose two orders of magnatude greater than the failure level of other microcircuits. The upper limit of total dose which will cause a TIC device to fail is still undefined. Additional work in this area should be undertaken.

The future of TIC devices is very bright. They should and will be used to compliment modern integrated circuitry in critical weapons, communications and space systems.

APPENDIX

TEST EQUIPMENT LIST:

1. Hewlett Packard 6209B DC Power Supply:
   0-320V, 0-.1A

2. Hewlett Packard 6205B Dual DC Power Supply:
   0-40V, .3A/0-20V, .6A

3. Hewlett Packard Harrison 6200B DC Power Supply:
   0-40V, .75A/0-20V, 1.5A

4. Keithley 617 Programmable Electrometer

5. Tektronix 7603 Oscilloscope
   7B85 delayed timing base, 7A26 dual trace

6. Tektronix 7904 Oscilloscope
   7B85 delayed timing base, 7A26 dual trace

7. Ohmite Ohm-Ranger
   resistance range 1 ohm thru 11,111,110 ohms

8. Weller Electronic Soldering Station

9. Tektronix C-5C Oscilloscope Camera

10. Tektronix C-51 Oscilloscope Camera

11. SOLA 115 V AC Rectifier/Inverter

12. Textronix Type 576 Curve Tracer

13. WAVETEK General Purpose VCG

LIST OF REFERENCES

1. Lynn, D. and McCormick, L., et al., "Progress in Radiation Immune Thermionic Integrated Circuits", LA-UR-84-527. (unpublished)

2. Glasstone, S.and Dolan P. J., The Effects of Nuclear Weapons pp.1-12, United States Department of Energy and Energy Research and Developement Administration, 1977.

3. Grover G. E. "Basic Radiation Effects in Electronics Technology", IEEE.1981 Annual Conference on Nuclear and Space Radiation Effects,pp.31-40, 1981

4. Interview with Lynn, D. at Los Alamos National Laboratory, October 6, 1985.

5. Eisberg, R. and Resnick, R., Quantum Physics of Molecules, Solids, Nuclei, and Particles, John Wiley and Sons, 1974.

6. Chaffin R. J., Microwave Semiconductor Devices: Fundamentals and Radiation Effects, John Wiley and Sons. 1957.

7. Eherenberg, W. and Gibbons, D. J., Electron Bombardment Induced Conductivity, Academic Press, 1981.

8. Vook, F.L., Radiation Effects in Semiconductors, Plenum Press, 1968

9. Arnold, G. W., and Compton, W. D., "Threshold Energy for Lattice Displacement in α-Al_2O_3", Phys. Rev. Let. V.4, No.2, 15 January 1960.

10. Cahn, J. H., "Irradiation Damage in Gremanium and Silicon due to Electrons and Gamma Rays", J. Appl. Phys., No. 30 p. 1310 1959.

11. Dienes, G. J., and Vinyard, G. H., Radiation Effects in Solids, Interscience Publishers, 1957.

12. Enge, H. A., Introduction to Nuclear Physics, p.185, Addison-Wesley, 1966.

13. Berger, M. A., and Seltzer, S. M., "Stopping Powers and Ranges of Electrons and Positrons", NBSIR 82-2550 1982.

14. Berard, R. W., and Traverso, T. J., Neutron Form Factors from Elastic Electron-deuteron Scattering Ratio Experiments at Very Low Momentum Transfers, Masters thesis, Naval Postgraduate School, Montery California, June 1973.

15. Rudie, N. J., Principals and Techniques of Radiation Hardening, 2d ed., V.1, pp. 2-1,2-42, Western Periodicals, 1980.

16. Cleveland, D. G., "Dose Rate Effects in MOS Microcircuits", IEEE Trans.Nucl. Sci., Vol. NS-31, No.6, pp. 1348-1353, December 1984.

17. Long, D. M., "Hardness of MOS and Bipolar Integrated Circuits", IEEE Trans. Nucl. Sci., NS-27 No. 6, pp. 1674-1679, December 1980.

18. Pease, R. L. et al., "Total Dose Effects in Recessed Oxide Digital Bipolar Microcircuits", IEEE Trans. Nucl. Sci., Vol. NS-30, No. 6, pp. 4216-4223, December 1983.

19. Raymond, J. P., "Environments, Failure Mechanisms,and Simulation of Radiation Effects on Microelectronic Componants", IEEE 1985 Nuclear and Space Radiation Effects Conference., pp. 1.30-1.35, July 1985.

INITIAL DISTRIBUTION LIST

		No. Copies
1.	Defense Technical Information Center Cameron Station Alexandria, Virginia 22304-6145	2
2.	Library, Code 0142 Naval Postgraduate School Monterey, California 93943-5100	2
3.	Prof. F. R. Buskirk, Code 61Bs Department of Physics Naval Postgraduate School Monterey, California 93943-5100	6
4.	Prof. J. R. Neighbours, Code 61Nb Department of Physics Naval Postgraduate School Monterey, California 93943-5100	1
5.	Lt. W. R. Arguello P. O. BOX 45 Declo, Idaho 83323	4
6.	Mr. M. P. Arguello P. O. BOX 45 Declo, Idaho 83323	1
7.	Dr. D. Lynn E-11 Division Los Alamos National Laboratory Los Alamos, New Mexico 87545	1
8.	D. Snyder, Code 61 Department of Physics Naval Postgraduate School Monterey, California 93943-5100	1
9.	Mr. Jim Chatburn P. O. Box 26 Albion, Idaho 83311	1
10.	Mrs. Stan Fredrickson 1520 Spring Run Drive Salt Lake City, Utah 84117	1

216066

Thesis
A6543 Arguello
c.1 The radiation effects of high energy electrons upon thermionic integrated circuits.

14 MAY 80 35153

216066

Thesis
A6543 Arguello
c.1 The radiation effects of high energy electrons upon thermionic integrated circuits.

thesA6543
The radiation effects of high energy ele
3 2768 000 69066 3
DUDLEY KNOX LIBRARY